DISCLAIMER

This report was prepared as an account of work sponsored by an agency of the United States Government. Neither the United States Government nor any agency thereof, nor any of their employees, makes any warranty, express or implied, or assumes any legal liability or responsibility for the accuracy, completeness, or usefulness of any information, apparatus, product, or process disclosed, or represents that its use would not infringe privately owned rights. Reference herein to any specific commercial product, process, or service by trade name, trademark, manufacturer, or otherwise does not necessarily constitute or imply its endorsement, recommendation, or favoring by the United States Government or any agency thereof. The views and opinions of authors expressed herein do not necessarily state or reflect those of the United States Government or any agency thereof. Reference herein to any social initiative (including but not limited to Diversity, Equity, and Inclusion (DEI); Community Benefits Plans (CBP); Justice 40; etc.) is made by the Author independent of any current requirement by the United States Government and does not constitute or imply endorsement, recommendation, or support by the United States Government or any agency thereof.

GA-A30331

FUSION PILOT PLANT AND ITER SCENARIOS AND CONTROL

By

A. Garofalo, P. Bonoli, D. Brower, Z. Sun, and X. Xu

Report prepared for the U.S. Department of Energy,
Office of Fusion Energy Sciences, under Award Number DE-SC0010685,
in compliance with Section B of DOE F 4600.2, Federal Assistance Reporting Checklist.

This material is based upon work supported by the U.S. Department of Energy,
Office of Fusion Energy Sciences, under Award Number DE-SC0010685

GENERAL ATOMICS PROJECT A30405

AUGUST 2025

GENERAL ATOMICS

FUSION PILOT PLANT AND ITER SCENARIOS AND CONTROL

Funding Opportunity Announcement Number	DE-FOA-0002702
DOE/Office of Science Program Office	Fusion Energy Sciences
DOE/Office of Science Program Office Technical Contact	Dr. Matthew Lanctot
DOE Award Number	DE-SC0010685
Funding Period	August 2022 – August 2025
Collaborating Institutions and Principal Investigator (PI) Names	**Andrea Garofalo** **General Atomics (GA)** **Lead PI** Paul Bonoli Massachusetts Institute of Technology (MIT) Co-PI David Brower University of California Los Angeles (UCLA) Co-PI Eugenio Schuster Lehigh University (LU) Co-PI Zhen Sun Princeton Plasma Physics Laboratory (PPPL) Co-PI Xueqiao Xu Lawrence Livermore National Laboratory (LLNL) Co-PI

Report prepared for the U.S. Department of Energy, Office of Fusion Energy Sciences, under Award Number DE-SC0010685, in compliance with Section B of DOE F 4600.2, Federal Assistance Reporting Checklist.

This material is based upon work supported by the U.S. Department of Energy, Office of Fusion Energy Sciences, under Award Number DE-SC0010685.

TABLE OF CONTENTS

LIST OF FIGURES

1. Executive Summary

Project Objectives. The principal goals of this renewal project were to develop key physics understandings and control solutions necessary for the realization of a steady-state fusion reactor by adapting high performance plasma scenarios from DIII-D to long pulse operation on the Experimental Advanced Superconducting Tokamak (EAST) in Hefei, China. Specific research objectives include the development of physics and control solutions necessary for demonstrating disruption-free long-pulse plasmas at high physics performance sustained simultaneously with the capability of handling the plasma exhaust and plasma-wall interactions using reactor-relevant materials surrounding the plasma. This was highlighted as a key strategic goal by both the 2020 FESAC Long Range Plan [FESAC 2020] and the 2019-2020 APS-DPP Community Planning Process report [APSCPP 2020].

Project Team. The project team has been comprised of scientists from six U.S. institutions led by General Atomics (GA), working in close coordination with the team at EAST. In addition to GA, the project team included Lawrence Livermore National Laboratory (LLNL), Lehigh University (LU), the Massachusetts Institute of Technology (MIT), Princeton Plasma Physics Laboratory (PPPL), and the University of California Los Angeles (UCLA).

Project Elements. The project consisted of three interrelated tasks, each divided into several subtasks. The main tasks are **1. Prediction and Demonstration of High Performance Steady-State Scenarios**, with the goal of adapting selected scenarios developed both experimentally on DIII-D and in simulation, on EAST long pulse experiments; **2. Control for Disruption-free Scenario Realization and Robust Sustainment**, with the goal of developing and implementing new control algorithms and architectures required for the robust realization and sustainment of long-pulse advanced scenarios; **3. Power Handling and Core-Edge Integration**, with the goal of developing and validating plasma edge and advanced divertor solutions and related predictive capabilities to integrate divertor heat and particle handling with core performance requirements for the long pulse plasma scenarios.

Project Results. Working synergistically with US domestic research, the partnership with EAST has had a large impact on world fusion efforts. For example, a major challenge for the world MFE program is the heating of the plasma ions using RF-only heating actuators. Most concepts for a future fusion pilot plant indeed assume that this will be possible. Yet, the long pulse experiments on EAST, including the recent world record for H-mode plasma duration in a tokamak (1066 seconds), have shown that achieving high $T_i \sim T_e$ is a major challenge using RF-only. EAST has a full complement of heating and current drive (H&CD) actuators to investigate this issue, probably the most complete set of actuators in the world. Our work in **Task 1** identified ITG

turbulence as the mechanism limiting the ion temperature in the long pulse EAST plasmas, and demonstrated that strong gas injection in a broad current density profile (high q_{min}) is a possible solution to overcome this challenge, and improve confinement quality. The associated physics model of turbulence suppression by high α_{MHD} and low magnetic shear was validated successfully through coordinated high poloidal-beta experiments on EAST and DIII-D first, and on KSTAR more recently. This new understanding is expected to have a crucial impact on the operation of ITER in the safer regime of lower plasma current, and on the realization of compact and economical fusion reactors in the future. In support of these experiments, our research efforts in **Task 1** have also focused on improving the understanding and modeling of RF actuators that can provide off-axis current drive for reducing the magnetic shear at mid-radius for turbulence suppression. The work under **Task 2** has yielded advancements in Disruption Prediction Modeling and in several long-pulse control challenges: an integrated deep learning model that combines disruption prediction with the identification of multiple precursor events; development, simulation and testing of machine-portable, real-time adaptive feed-forward optimization for shape control; and development and improvement of real-time proximity-to-instability control for disruption avoidance (especially VDEs) and its connection to fault handling. In addition, results from **Task 2** will be discussed in a separate report by the Lehigh University group. Work in **Task 3** has advanced the use of impurity powder injection as a key tool for developing integrated, long-pulse scenarios. For example, a novel dynamic wall conditioning technique, utilizing real-time feedback control of lithium powder, was instrumental in achieving the record-duration H-mode discharge by actively managing fuel recycling and impurity influx. Complementing these efforts, our work in **Task 3** has produced foundational insights into the physics and control of small and grassy ELM regimes, SOL broadening, and detachment: the identification of fluctuation intensity flux (Γ_ε) as a predictive metric for SOL width expansion, the development of physics-informed neural network surrogate models for divertor detachment behavior; the validation, in EAST impurity seeding experiments, of predicted pedestal transitions to grassy ELM regimes and to full detachment with nitrogen injection.

More details on the project activities and research findings throughout the entire period of funding are given in the following subsections for each collaborating institution, except for Lehigh University providing a separate report.

2. GA Contribution (PI: A.M. Garofalo)

Accomplishments in General Atomics execution of tasks under the Fusion Pilot Plant and ITER Scenarios and Control International Collaboration Grant include:

I. Task 1: Prediction and Demonstration of High Performance Steady-State Scenarios

I.1. Introduction

EAST provides unique opportunities for the study of long-pulse scenario development and control in reactor-relevant conditions. Currently, EAST is the only facility in the world that can enable US scientists to pioneer the development of physics and control solutions necessary for long-pulse at high physics performance with simultaneous reactor-relevant effects of torque-free actuators, metal walls and divertors, reactor-capable diagnostics and control systems. No comparable capabilities are foreseen in any facility in the near future, until ITER.

Figure 1 illustrates the progress of long pulse, steady state tokamak operation on EAST over the last 15 years, including the present world record duration of 1066 s H-mode plasma, achieved in January 2025 [X. Gong et al, IAEA FEC 2025]. Long pulse operation in EAST is achieved via a high-β_P scenario using only RF sources for heating and current drive (lower hybrid, electron cyclotron, and ion cyclotron wave H&CD) and a tungsten divertor.

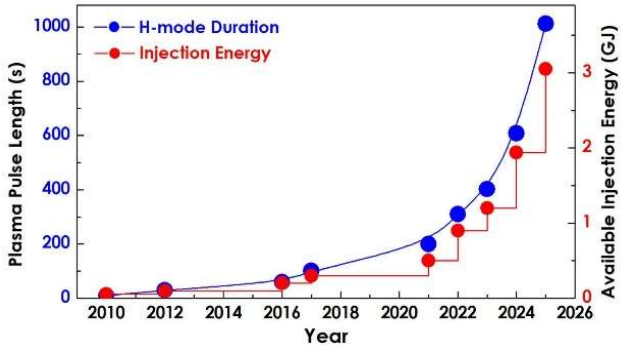

Fig. 1. Progress of long pulse operation for H-mode in EAST

These experiments have demonstrated advancements in the physics understanding and control of the core, edge, and boundary plasma, as well as in RF and metal wall technologies. However, these experiments have also highlighted that achieving high $T_i \sim T_e$ using RF-only, which is a requirement for future fusion pilot plants (FPPs), is a major challenge for the tokamak approach to fusion electricity.

GA's work [S. Ding et al, "Strategy for Developing Internal Transport Barriers at Large Radius in High Poloidal Beta Plasmas on EAST", APS DPP Meeting 2021, abstract id.CP11.012] using gyrokinetic and gyrofluid modeling tools showed that the core plasma of these long pulse

EAST experiments is trapped at low α_{MHD} (a normalized pressure gradient) by ITG (ion temperature gradient) and KBM (kinetic ballooning modes) turbulence, as shown in Figure 2 (left). This work also showed that lower magnetic shear (ŝ) at mid radius is essential for increasing the local pressure gradient using RF heating only, thus creating a large radius internal transport barrier and improving the energy confinement quality for both ions and electrons. As shown in Figure 2 (right), increasing the injected heating power is predicted to have nearly no impact on the mid-radius pressure gradient, unless the q-profile is modified to reduce the mid-radius magnetic shear. These predictions have been validated in recent EAST experiments [S. Ding et al, *Phys. Plasmas* **32**, 022502 (2025)].

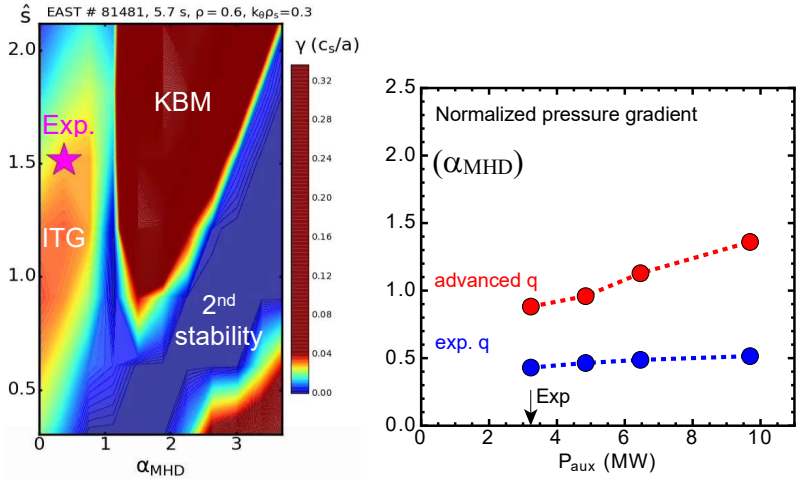

Fig. 2. (Left) 2D scans of linear growth rate (color coded) of most unstable turbulent mode (calculated by CGYRO at ρ=0.6) vs. α_{MHD} and magnetic shear. Magenta star shows the experiment data point. (Right) Predicted α_{MHD} at q=0.55 vs. auxiliary heating power with different q-profiles: experimental q-profile (blue), and advanced q-profile with q_{min}>2 and lower magnetic shear at mid-radius (red).

I.2. Test "Early Heating" Path to High-q_{min} Current Profile for Large-radius ITB

Early EC heating was used for the first time on EAST in a high-β_P scenario experiment led by A. Garofalo (remotely) on June 26, 2022. The early ECCD application (during the plasma current ramp-up) produced broad current profiles, broader with the injection further off-axis. This was shown both by the reconstructed internal inductance (li), and by POINT measurements of the internal magnetic field structure. Using TRANSP, we carried out extensive time-dependent transport modeling of these early heating experiments. The modeling yielded excellent match of the experimentally measured electron temperature profiles, and revealed the formation of a reversed shear profile with q_{min}>2. The modeling also predicted that strong off-axis EC heating will cause the LHCD profile to peak off-axis. This could help sustain the high q_{min} profile, together with additional heating power.

Following the modeling guidance, new EAST high-β_P scenario experiments were led by Wilkie Choi (remotely) on July 20 and 28, 2023. These experiments successfully produced higher q_{min} plasmas with lower internal inductance, and applied additional power using LHW, NBI, and ICRF. The LHCD did not perturb the low li state, consistent with the modeling predicting off-axis deposition. But the broad current profile from the early ECCD was lost after the injection of high NBI+ICRF power. Also, because of the off-axis injection of ECCD, the heating impact was strongly reduced, and the energy confinement quality was quite poor, therefore the injected power was still not sufficient to increase beta and sustain the high q_{min} profile via the bootstrap current. These results suggested that future efforts on this path would require the availability of more EC power, for simultaneous on-axis ECH to increase beta, and off-axis ECCD for achieving high q_{min}.

Since high-power on-axis ECH is also essential on EAST for control of the tungsten accumulation in the core during long-pulse plasmas, the requirement to move some EC power off-axis for current profile tailoring led us to start new research to investigate the use of ICRF for tungsten impurity control, to replace the on-axis ECH. This research was enabled by the addition to the team of a post-doctoral scientist, Shengyu Shi, in November 2023.

I.2.1. Using ICRH for Tungsten Control in EAST

GA's studies demonstrated that ion cyclotron resonance heating (ICRH) effectively mitigates core tungsten (W) accumulation in high-performance H-mode plasmas. The primary mechanism involves ICRH-induced suppression of plasma rotation, which weakens the neoclassical inward pinch. In contrast, the hydrogen minority isotropic temperature exhibits minimal influence on W transport. These findings have been presented at the 2024 US-EU Transport Task Force (TTF) and submitted to the 2025 IAEA Fusion Energy Conference (FEC). This work is also published in *Nuclear Fusion* [Zhen Zhou, Shengyu Shi, et al., 2025, Nucl. Fusion 65 036004], contributing to EAST's goal of sustaining high-performance plasmas with minimal impurity accumulation.

To further investigate the physics behind ICRH-driven tungsten control and identify optimal operating regimes, we carried out a dedicated experimental campaign on EAST (Proposal: "Study on tungsten impurity transport under ICRH heating in EAST H-mode plasma," dated 2024.05.26). The scans covered toroidal field strengths (11-12 kA), H/D ratios (2-11%), and magnetic configurations including gap-out scenarios. Analysis is being carried out by EAST personnel. Furthermore, in order to validate our modeling of impurity transport, we performed a detailed analysis of impurity transport in DIII-D hybrid plasmas, to take advantage of the excellent profile measurements available at DIII-D. The experimental results showed that high-Z impurity accumulation does not occur in either low- or high-density hybrid regimes. Consistent with the experimental results, our modeling further revealed that the lack of impurity accumulation in these plasmas can be primarily attributed to a dominant outward neoclassical convection velocity, driven

by the temperature screening effect (see Figure 3). These modeling results will be submitted for publication shortly.

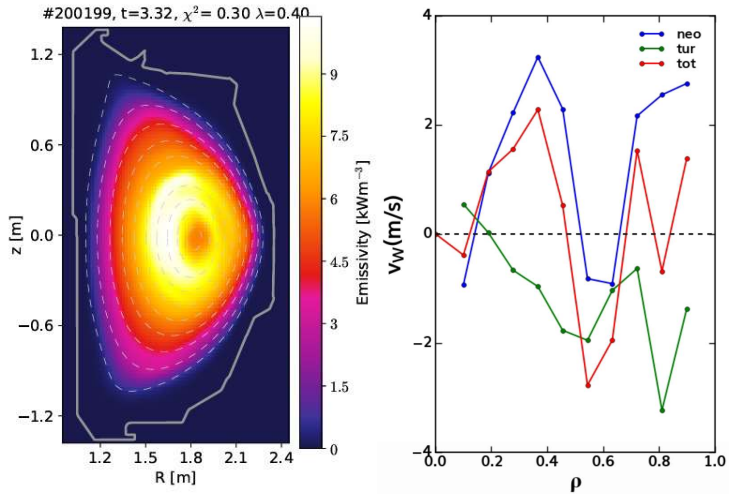

Fig. 3. (Left) Tomographic reconstruction of the SXR emissivity (the different dashed contour lines represent ρ=0.1 to 1) in DIII-D shot #200199 at t~3.3s. (Right) Radial profile of predicted convection velocity for W using NEO and TGLF. Legends 'tur' and 'neo' denote the turbulent and neoclassical contribution, respectively. 'tot' means the total, which is the sum of neoclassical and turbulent contributions.

I.3. Large-Radius ITB Formation Using "Late Heating" Path to High-q_{min} Current Profile

An EAST experiment on August 9, 2023, led by Wilkie Choi and Siye Ding (remotely) investigated a different approach to broad current profile formation in the high-β_P scenario, which did not use early heating. This approach used a lower plasma current target, and injected high heating power (> 10 MW) all during the plasma current flat-top, at high density. Using on-axis ECH improved the energy confinement quality and led to high normalized beta (~2.5) and very high poloidal beta (~4) with a broad current profile (internal inductance li~0.6) in fully noninductive conditions. MSE constrained q-profile reconstructions suggested a stationary q_{min}>2. This path to high q_{min} would be preferable for a reactor, compared to the early heating path that might require high power injection before the plasma enters the diverted configuration, and thus could overheat the limiters. New modeling is necessary to understand the dynamics of this approach to a low li plasma state.

This low li plasma state was used for an attempt at triggering a large radius ITB by a combination of a strong impurity gas puff plus a brief 2nd ramp-up of the plasma current (I_P). This approach was proposed based both on modeling of EAST plasmas by Siye Ding, and extensive time-dependent modeling carried out in a sub-contracted effort by M. Kotschenreuther and D. Hatch of ExoFusion in Austin Texas. The time-dependent modeling was carried out using the FASTRAN code, and suggested the use of a 2nd Ip ramp-up to further reduce the magnetic shear

at large radius, in combination with deep particle fueling using pellets to increase the density gradient at large radius, and with impurity injection to increase the impurity gradient at large radius (density gradient and impurity gradient were predicted to enhance the impact of alpha-stabilization of turbulence).

The experiment did not have pellet fueling available. However, it was able to use a brief, 2nd I_P ramp-up in combination with a strong but brief puff of Argon gas. With these actuators, the ion temperature was nearly doubled, and remained elevated for several seconds after the Ip ramp and impurity injection had ended, overcoming a long-standing limitation in long pulse operations.

The experiment showed that a large radius ITB was triggered and sustained by its own bootstrap generated current, with a sustained Greenwald fraction (f_{Gr}=line-averaged electron density/Greenwald density) ~0.9. These results confirmed the predict-first transport simulations and earned a post-deadline invited talk at the 2023 APS-DPP meeting, delivered by Siye Ding, and published in Phys. Plasmas [S. Ding et al, *Phys. Plasmas* **32**, 022502 (2025)]. More generally, these results confirmed our understanding of the physics of alpha-stabilization of turbulence, which is at the heart of progress obtained also in DIII-D experiments, where f_{Gr} above 1 was achieved simultaneously with normalized confinement (H_{98y2}) well above 1, as required in fusion reactor designs but never before verified in experiments. These results were published in a paper in Nature [S. Ding et al, Nature **629**, 555 (2024)].

I.3.1. Understand Velocity Space Dynamics of EC + LH Waves Synergy

Time slice simulations using the ray-tracing code GENRAY and the 3D Fokker-Planck solver CQL3D have been performed to capture the phase space interactions of EC and LH waves. It is predicted that the localized EC deposition is able to create a population of fast electrons, which enhances the Landau damping of LH waves, partially concentrating the typical broad LH deposition profile. To investigate this predicted effect, an experiment was conducted on EAST on February 5, 2024, led by Wilkie Choi (remotely). In the experiment, scans between shots and during shot confirmed that movement of EC power indeed affects li and the HXR profile, indicating that the LHCD profile has been modified. While synergistic effects between EC and LH have been previously observed on EAST, this work demonstrates for the first time the possibility of using the EC to create a local population of fast electrons in the phase space, which the LH will preferentially damp on, in effect concentrating the LH power damping at the EC resonance layer.

The combination of the steerable ECCD and efficient LHCD provides a new tool for broadening and tailoring steady-state current profiles, which opens new avenues in scenario development for advanced tokamak concepts that require efficient off-axis current drive. Based on this experiment and related simulations, Wilkie Choi obtained an invited talk at the 2024 APS-DPP

meeting in Atlanta, Georgia, and an invited talk at the 2024 AAPPS-DPP meeting in Malaacca, Malaysia.

I.4. Rescoped Work on Large-Radius ITB Scenario on KSTAR

A high-β_P experiment led by S. Ding et al. was performed on KSTAR in February 2025. The purpose of the experiment was to establish internal transport barriers (ITB) at large radius, which have not yet been achieved in the high poloidal beta (β_P) scenario on KSTAR. The motivation is that despite all the achievements in the previous DIII-D high-β_P experiments, a few key issues of scenario development cannot be addressed on DIII-D, due to the limitation of the present DIII-D tokamak. One is the long-duration sustainment of large radius ITB, which is limited by the pulse length of DIII-D (5-6 s). The other is the scenario access and sustainment with metal wall. Both of these issues can be tested on KSTAR, if the scenario is successfully established. This experiment also represented a follow-up research after our high-β_P experiments on EAST, to further test the experimental approach we developed on EAST for triggering large-radius ITBs.

The results of the new high-β_P experiment on KSTAR were very promising, leading to an invited talk by our KSTAR collaborator Y. M. Jeon at the 4th International Fusion and Plasma Conference (iFPC-2025) in Daejeon, Korea, 2025, and an oral presentation, also by Y. M. Jeon, at the upcoming 30th IAEA Fusion Energy Conference (FEC 2025), Chengdu, China, 2025. The experiment consisted of two parts: the first part used an upper single null (USN) plasma shape configuration with strike point on the carbon divertor, for easier comparison with the DIII-D experiments, which used carbon divertor as well. The maximum available heating power (NBI+ECH) on KSTAR is about 8 MW. Such power level is similar to the DIII-D experiments, when the power is scaled for the smaller volume of KSTAR plasmas. The main goals of the scenario development were achieving a broad current density profile, triggering a large radius ITB by strong heating and fueling of the plasma.

The experimental results indeed showed lower l_i (~0.8) than the value in the previous KSTAR long-pulse high-β_P operation (~1.2), indicating success in broadening of the current profile. Improved β_N and a mid-radius (ρ~0.4) ion temperature gradient increasing with constant power and gas puffing rate are also observed, showing success in triggering an ITB. Detailed experimental waveforms and profiles are shown in Figure 4. However, it is important to note that the achieved performance/confinement in the KSTAR high-β_P experiment is lower than in the counterpart experiments on DIII-D. The profile gradient in T_i is not as strong enough and the ITB radius is not as large. Also, there is no sign of ITB in the T_e and n_e channels. The observations suggest insufficient α_{MHD} and/or not low enough magnetic shear at mid-radius.

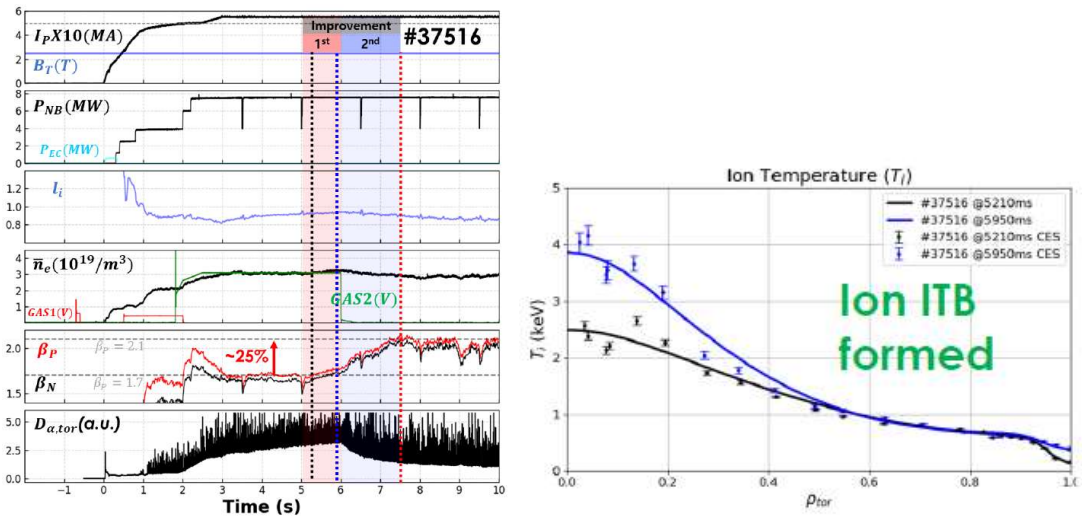

Fig. 4. (Left) Time histories of KSTAR #37516. (Right) T_i profiles from #37516 just before (t=5210 ms, black) and after (t=5950 ms, blue) ITB formation; Dots with error bars are measurements and solid lines are fits.

To investigate why the large-radius ITB did not appear in these recent KSTAR high-β_P plasmas, TGLF modeling with saturation rule SAT2 is employed to analyze the turbulent fluxes at mid-radius, such as ρ=0.55, in the discharge discussed above [S. Ding et al., 67th APS-DPP, 2025]. As shown in Figure 5 (left), the ion turbulent transport is mainly driven by an ion mode with peak amplitude at $k_y\rho_s$~0.6, while the electron turbulent transport has two drivers, including the same ion mode at low-k, and an electron mode at high-k ($k_y\rho_s \geq 2$). An $\hat{s}$-α scan is then carried out to uncover the transport features in the operational space adjacent to the experimental conditions. Here, $\hat{s}$ is the local magnetic shear and α refers to α_{MHD}, which is a normalized pressure gradient. As one can see in Figure 5, the $\hat{s}$-α scans show transport "mountains" due to instabilities near the experimental data point in both ion and electron channels. The fact that the transport mountains are localized on the higher α side of the experimental state, suggests that higher heating power would be easily dissipated by the excited turbulence, without increasing α. However, a path to higher hardly increase α would not encounter strong turbulence if $\hat{s}$ can be sufficiently reduced (<0.2 suggested by this modeling). The analysis supports the earlier hypothesis of insufficiently low magnetic shear at mid-radius, and suggests further efforts on broadening the current density profile in future coming KSTAR experiments.

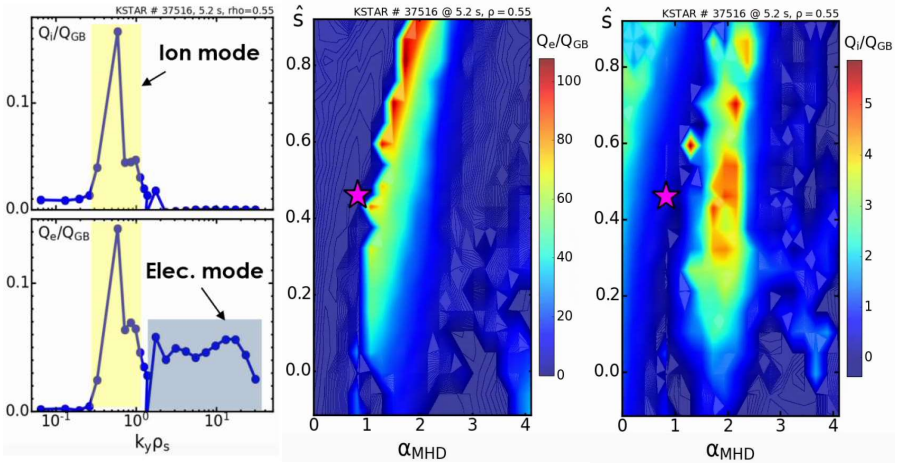

Fig. 5. (Left) Spectrum of heat fluxes in the ion channel (top) and electron channel (bottom); Yellow shaded areas highlight the feature of the modes that drives the heat fluxes; (Middle) $\hat{s}$-α scan for the electron heat flux based on equilibrium from KSTAR #37516 at t=5.2 s and ρ=0.55; (Right) $\hat{s}$-α scan for the ion heat flux based on the same equilibrium. Purple star in middle and right figure indicates the experimental data point.

The second part of the high-β_P experiment on KSTAR used a lower single null (LSN) plasma shape with strike point on the tungsten divertor. Strong interactions between plasma and the tungsten divertor in the early phase of the discharge were successfully avoided using expedients already developed by the KSTAR team, including a specially designed plasma shape and early divertor gas puffing. The discharges of this second part of the experiment also showed improved β_N and enhanced ion temperature gradient at ρ~0.4, which is very promising. Experimental waveforms and profiles from a typical discharge with LSN configuration and tungsten divertor are shown in Figure 6. Note that, similar to the USN results, the achieved performance/confinement is lower than in the counterpart DIII-D experiments. The key challenge is believed to be an insufficient broadening of the current density profile, as discussed above. Based on these recent experiments and modeling results, several new experiment proposals have been submitted to the KSTAR Research Opportunity Forum (ROF) in July, 2025, to further improve the scenario recipe and establish ITBs at large radius.

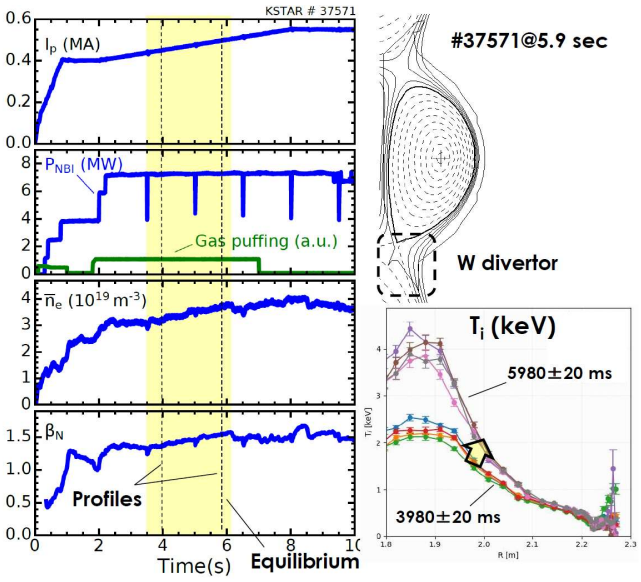

Fig. 6. (Left) Time histories of KSTAR #37571. (Right top) Equilibrium reconstruction at t=5.9 s. (Right bottom) T_i profiles just before and after the ITB formation.

II. Task 2: Control for Disruption-free Scenario Realization and Robust Sustainment

GA's work under Task 2 has yielded significant development and insight into several long-pulse control challenges: development, simulation and testing of machine-portable, real-time adaptive feed-forward optimization for shape control, and development and improvement of real-time proximity-to-instability control for disruption avoidance (especially VDEs) and its connection to fault handling.

II.1. Real-Time Feed-Forward Coil-Current Optimization Shape Control with the OCELOT Algorithm

The OCELOT (**o**ptimized **c**oil currents for **e**nhanced **l**ong-pulse **o**peration of **t**okamaks) algorithm aims to improve shape control in long-pulse tokamaks by replacing the feedforward component of coil current commands with a secondary feedback loop that uses model-based optimization to calculate optimal coil currents (see Figure 7). OCELOT was developed from a previous real-time feedforward algorithm originally implemented on KSTAR, but uses a more advanced model. Feedforward coil current commands are difficult to predict accurately prior to a shot, which places most of the control burden on the feedback shape control algorithm (e.g. isoflux). As shots become longer and feedforward predictions become less accurate, it has been found that high integral gains become necessary to maintain good shape control; these high gains open up the possibility of a variety of issues, including control instabilities and windup problems. Replacing the inaccurate feedforward commands with optimized commands in real time places less burden on isoflux, allowing for lower integral gains without compromising the shape control.

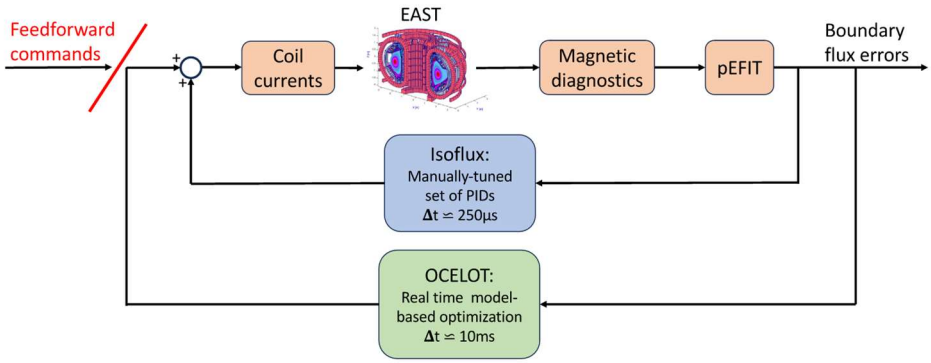

Fig. 7. Block diagram of EAST's shape control system with OCELOT implemented.

The biggest difference between the original real-time feedforward algorithm and OCELOT is the model used by the real-time optimizer. The previous real-time feedforward implementation used a model that was constant in time, and assumed a specific shape target and plasma current profile. The model used by OCELOT varies in time and takes into account both changes in the shape targets and in the current profile, in real-time. Simulation results comparing the flux at each boundary control location and the magnetic field components at the target X-point predicted by the OCELOT model to measured data from EAST shot 94421 show very good agreement (see Figure 8).

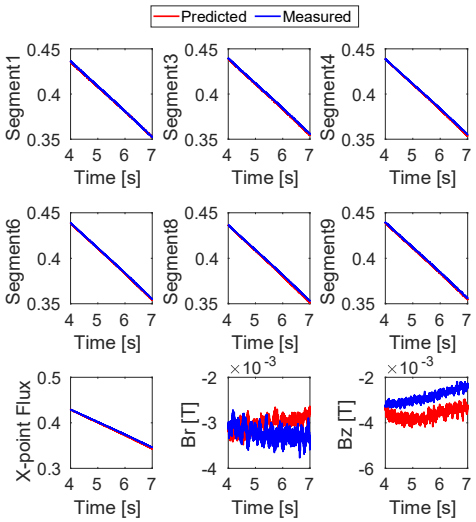

Fig. 8. Simulation results for the OCELOT model tested on EAST shot 94421.

The other notable difference between the previous real-time feedforward and OCELOT is in the method within the PCS (plasma control system) implementation. The new OCELOT PCS implementation is written entirely in C (as opposed to the previous code generated from Simulink). The C code was written in a way to make it as easy as possible to port between different machines

(see Figure 9). This includes the implementation of both a modular and machine-portable larger OCELOT algorithm for model evaluation as well as a machine-portable optimizer it uses.

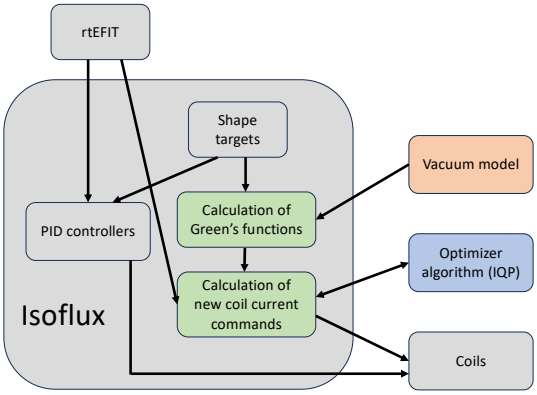

Fig. 9. Diagram of the PCS implementation of OCELOT, where the gray boxes represent unchanged code, the green boxes represent machine-independent code, the orange box represents machine-dependent code, and the blue box represents machine- and algorithm-independent code.

The OCELOT algorithm was implemented and in the testing stages to prepare for EAST experiments in 2025 Spring, and was on track for experiments. An experimental proposal was likewise submitted to test these capabilities in the Spring 2025 campaign. However, due to the discontinuation of collaboration on EAST experiments and data, this development and the experiment had to be discontinued per DOE's request. To rescope for the remaining effort, development and simulation were done simulating and analyzing related work on KSTAR.

II.2. Rescoped Work on Real-Time Feed-Forward Techniques on KSTAR

Experiments were run in the 2024-2025 KSTAR campaign to test the initial implementation of the OCELOT algorithm as part of work on a different grant award. In those experiments, some unexpected behavior with the control was observed. For the rescoped effort on this grant, this behavior was investigated with simulation to try to isolate the source of the instability, and to try to debug and tune.

Sixteen shots were run in 8 different morning Ohmic sessions over the course of two months in the 24/25 Winter KSTAR campaign using OCELOT. A number of PCS implementation issues were identified and fixed throughout the experiments, leading to the final two shots in which OCELOT calculated the optimal coil currents correctly and sent requests to the coils successfully. These shots uncovered an instability in the control scheme that led to disruptions 0.5-1s after OCELOT was enabled. Figure 10(a) shows the growth of the instability in discharge 37492, which ultimately ended in disruption.

The instability was replicated in simulation using GSevolve with the PCS in the loop (see Figure 10(b)). The simulation work has rule out a number of potential causes of the instability,

including improper tuning of the weights used by the optimizer and high integral gains in isoflux interacting poorly with OCELOT. Exploration of other potential causes (e.g., delays in the coil reacting to commands) is ongoing, with the hope that the instability will be identified and mitigated before the next experimental campaign.

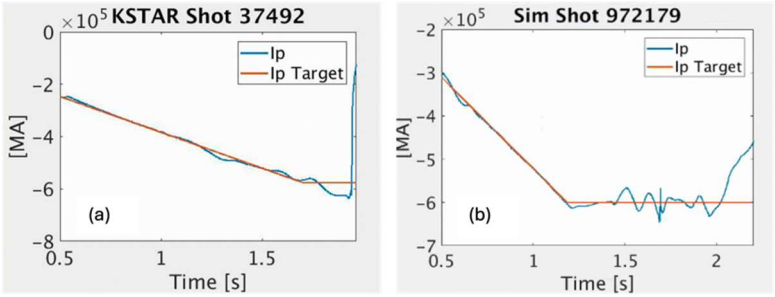

Fig. 10. Plasma current trace showing instability and disruption with OCELOT turned on in experiment (a) and in simulation (b).

II.3. Proximity Control for Disruption Prevention

At its base, Proximity Control is a method of disruption prevention taking advantage of early warnings from real-time stability calculations and monitoring nearness to known stability limits. The Proximity Control algorithm is in use on D3D and KSTAR, and was in the process of porting to EAST. Figure 11 gives a conceptual layout for the design of the Proximity Controller, used for mapping real-time stability metrics to control targets for avoidance. A workflow applying real-time shape modifications to avoid VDEs based on a real-time VDE growth rate is outlined in the figure by following the blue arrows.

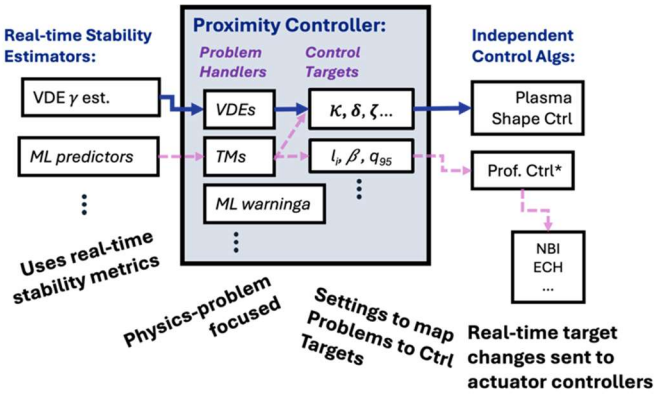

Fig. 11. Conceptual layout of the Proximity Control algorithm, with workflow of VDE prevention control following blue arrows. Real-time stability estimators are taken as inputs, processed for decision making on modifying control targets, and the modifications to the targets are sent to independent actuator algorithms to use.

For the specific case of VDE prevention, updated analysis of historical data found VDE growth-rate limits in previous runs with default vertical controller tuning to be ~250/s. This

provides the needed limit for use in experiments to have the proximity controller avoid VDEs, and is used to decide a reference level above which the controller will be permitted to take action. Figure 12 gives an example high fitted growth-rate from a historical VDE experiment to be used for this purpose. The updated analysis method performs growth rate fits over a two dimensional scan of the start and stop times of the signals to fit as well as calculates the res-norm of over the range to help avoid picking times too late when the evolution is highly non-linear.

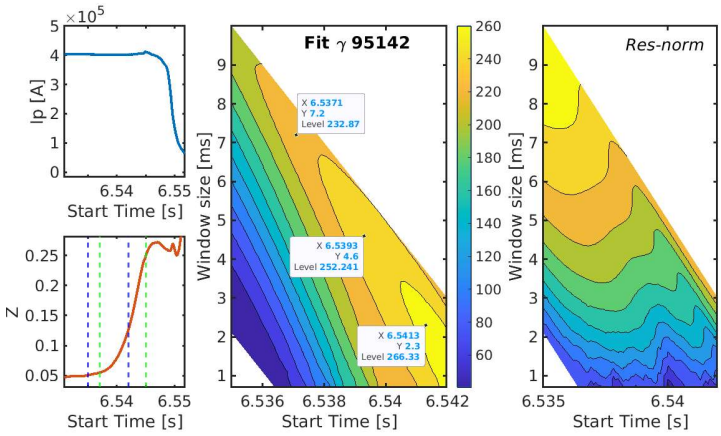

Fig. 12. Fit to experimentally measured VDE growth rate from historical data identifying high end VDE growth rate of order 250/s.

The design and implementation of the Proximity Controller is similar on EAST to other devices, but requires additional consideration to modify shape targets on EAST due to their use of a GPU-based rt-efit and related particulars of the isoflux implementation on EAST. The workflow was planned to test using the real-time VDE growth-rate estimation generated by EAST's GPU version of rt-efit as the input stability metric. The coding of the algorithm on EAST was on track to be ready in time for experiments in the Spring 2025 campaign, including with the real-time shape modifications added to isoflux. An experimental proposal was developed and submitted to EAST to test these new tools and methodologies. However, due to the discontinuation of collaboration on EAST experiments and data, this development and the experiments had to be discontinued per DOE's request. To rescope for the remaining effort, development and simulation were done on related work on KSTAR.

II.4. Rescoped work on related Proximity Control on KSTAR

For the rescoped effort on this grant, the KSTAR Proximity Controller was upgraded to test more intelligent algorithmic handling of when stability problems require escalation to the level of fault handling from proximity control. The KSTAR implementation/port of the proximity controller was used in disruption avoidance experiments in Winter 2024/2025 KSTAR campaign, including application for VDE avoidance. It was able to successfully avoid VDEs during flat-top

in those discharges. However, when it reached ramp-down the proximity controller could not adjust fast enough to continue regulating m_s. In cases just like this, it would be best if the Proximity Controller could recognize that the stability problem in question is no longer being adequately controlled, despite the interventions it has already taken, and escalate the problem to fault handling procedures to prevent imminent disruption (early shutdown, mitigation, etc.). New logic was added to the KSTAR implementation of the proximity control algorithm for just this purpose and tested in simulations: recognizing problem escalation beyond control adjustment to fault handling.

The proximity controller was upgraded to check if stability metrics are continuing to grow despite intervention, and then escalate the problem to fault handling. The proximity controller was connected to the Alarms algorithm of the KSTAR PCS to warn the Alarms when a stability problem is no longer under control, and to induce shutdown or mitigation for machine safety. Figure 13 gives an illustration of the updated logic added to the Proximity Controller implemented here: the red arrow and boxes indicating the problem escalation and request for shutdown from the PCS Alarms category.

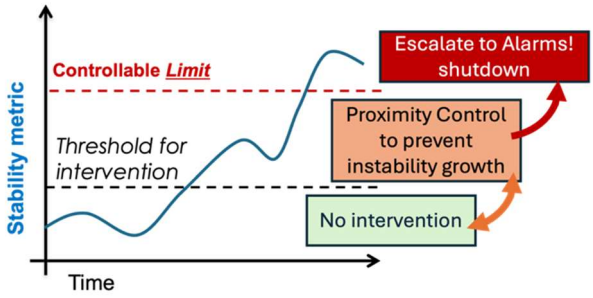

Fig. 13. Updated logic added to the KSTAR implementation of the Proximity Controller to handle problem escalation and communication to the Alarms algorithm to shutdown for device safety.

The design and implementation was completed and tested in TokSys datasim simulations based on data from the previous KSTAR experiments (based form discharge 36140). Figure 14 shows the results of the control simulations where the discharge was first programmed to ramp elongation until a VDE was induced. The first simulation repeats the original setup from the experimental shot (blue), and the second repeats the simulation with the new upgrades enabled (dotted dark orange). The simulation repeats the actions of the PCS exactly, with the important exception of Figure 14(c): the PCS alarms trip, successfully showing the new feature would have fired the mitigation in experiment.

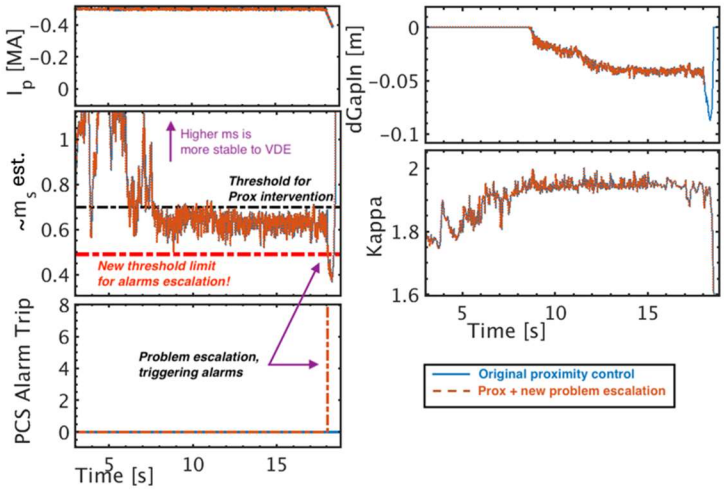

Fig. 14. Example simulation of KSTAR PCS using the upgraded PCS proximity control algorithm to recognize when an instability is continuing to grow despite current interventions, and to escalate to problem to fault response handling. (a) Ip, (b) marginal stability estimator value, (c) PCS alarm trip (alstripped), (d) requested change in gap-in from proximity controller, (e) elongation.

Figure 14(b) shows the real-time m_s estimate as well as the reference/threshold for the Proximity Controller to intervene, and the lower threshold estimating the disruption limit. In the original experiment and likewise repeated in the simulations performed here m_s drops below the threshold for intervention around 8s, and soon the proximity controller begins to take action by requesting changes to the plasma shape, specifically by decreasing elongation and reducing gapin (provides non-linear coupling via wall stabilization). After about t=9s, the m_s stability factor has been successfully regulated and prevented from dropping further, which saved the discharge in the experiment. However, at approximately 18s (when shutdown begins), the proximity controller loses control of m_s and it drops dangerously low. With the new problem escalation capability enabled, the controller recognizes the issue at t=18.05s and commands the alarms category to perform emergency shutdown or fire mitigation as indicated in the alarm trip signal "alstripped" in Figure 14(c). The team plans to test this new functionality in future experiments on KSTAR if possible.

III. Task 3: Power Handling and Core-Edge Integration

GA's work under Task 3 focused on characterizing pedestal stability and transport in H-mode plasmas and generating experimental data for testing and validation of the BOUT++ modeling tool.

An EAST experiment was led by Huiqian Wang (remotely) on July 31, 2023. The experiment aimed to test and validate BOUT++ simulations. These BOUT++ simulations have predicted that small ELMs with higher turbulence intensity flux broaden the heat flux width, consistent with theory and previous experimental observations. The machine ran very well, with reliable power

from NBI, ECH, and LHW. The experiment succeeded in reproducing high-frequency small ELM discharges, and also successfully changed the ELM behavior via several scans including Ip, torque, density. Lots of profiles data as well as fluctuations were obtained, including the turbulence intensity flux, Reynold stress, velocities, etc. The ELM crash process was successfully monitored using the gas puff imaging (GPI) diagnostic. In summary, we obtained a lot of experimental data including no-ELM, small ELM, and large ELM phases, which contributed to the model validation efforts by our LLNL collaborators, and provided references for further experiments.

IV. Presentations and Publications

Publications:

- S. Ding, A.M. Garofalo, H.Q. Wang, et al, "Turbulence suppression in plasmas around the Greenwald density limit on EAST and DIII-D", *Phys. Plasmas* **32**, 022502 (2025)
- S. G. Baek, M. H. Li, W. Choi, P. T. Bonoli, B. J. Ding, A. Garofalo, and G. M. Wallace, H. Xu, Q. Zang, "Modeling study of synergistic effects between lower hybrid and electron cyclotron current drive on EAST", Nucl. Fusion 65, 056003 (2025)
- Zhen Zhou, Shengyu Shi, et al, "Tungsten impurity reduction by ICRH in a high power injection and high performance H-mode discharge on EAST", Nucl. Fusion 65, 036004 (2025).
- Ding, S., Garofalo, A.M., Wang, H.Q. et al. "A high-density and high-confinement tokamak plasma regime for fusion energy", Nature 629, 555–560 (2024), https://doi.org/10.1038/s41586-024-07313-3
- X. Gong on behalf of EAST Team and Collaborators, "Overview of recent experimental results on EAST tokamak", Nucl. Fusion 64, 112013 (2024).
- Juan Huang, et al, "Long-pulse high-performance H-mode plasmas achieved on EAST", Phys. Plasmas 30, 062504 (2023)
- Y.C. Hu, et al, "Gyrokinetic simulations of core turbulence and thermal transport in the high-βP discharge on EAST", Plasma Phys. Control. Fusion 65, 055023 (2023)
- K. Wu, Q.P. Yuan, D. Eldon, K.D. Li, Y.M. Duan, L.Y. Meng, L. Wang, H.Q. Wang, J.J. Huang, L. Zhang, Z.P. Luo, X.J. Liu, B. Cao, J.B. Liu, F. Ding, G.S. Xu, J.S. Hu, B.J. Xiao, G. Calabrò, P. Innocente "The first achievement of the double feedback control of the detachment in the long-pulse plasma on EAST", Nuclear Materials and Energy 34, 101398 (2023)
- Z. Wang, H. Wang, E. Schuster, Z. Luo, Y. Huang, Q. Yuan, B. Xiao, D. Humphreys, S.T. Paruchuri, "Implementation and Initial Testing of a Model Predictive Controller for Safety Factor Profile and Energy Regulation in the EAST Tokamak", 2023 American Control Conference (ACC), San Diego, CA, USA, 2023, pp. 3276-3281, doi: 10.23919/ACC55779.2023.10156588.

- Yunchan Hu et al, "Gyrokinetic simulations of core turbulence and thermal transport in the high βp discharge on EAST", Plasma Phys. Control. Fusion 65 055023 (2023)
- Yuntao Song et al, "Realization of thousand-second improved confinement plasma with Super I-mode in Tokamak EAST", Science Advances 9 eabq527 (2023)
- Siye Ding and Andrea Garofalo, "Progress in the development and understanding of a high poloidal-beta tokamak operating scenario for an attractive fusion pilot plant", Reviews of Modern Plasma Physics 7 4 (2023)
- X.Z. Gong et al, "Realization of Te0> 10 keV long pulse operation over 100 s on EAST", Plasma Science and Technology 25 022001 (2023)

Presentations:

- X. Gong et al, "Overview of Recent Experimental Results on EAST in Support of ITER New Research Plan", Overview Oral at the 30th IAEA Fusion Energy Conference (FEC 2025), 13-18 October 2025, Chengdu, China.
- Y.M. Jeon et al, "Development of High Poloidal Beta Scenario for Long-Pulse Operation in Collaboration Between DIII-D and KSTAR", Oral at the 30th IAEA Fusion Energy Conference (FEC 2025), 13-18 October 2025, Chengdu, China.
- Y. M. Jeon et al., "Advancing High Poloidal Beta Scenarios for Reactor-Relevant Long-Pulse Operation: A Collaborative Effort Between DIII-D and KSTAR", Oral at the 4th International Fusion and Plasma Conference (iFPC-2025), Daejeon Convention Center (DCC), Korea, June 9-13, 2025
- Shira Morosohk, et al, "Initial Results from the OCELOT Algorithm: A Re-implementation of Real-Time Feedforward Shape Control", Poster Presentation at the 4th International Fusion and Plasma Conference (iFPC-2025), Daejeon Convention Center (DCC), Korea, June 9-13, 2025
- A.M. Garofalo, et al, "High Density as an Avenue towards High Confinement Quality and Core-Edge Integration in Advanced Tokamaks", Invited talk at the 2nd IAEA Technical Meeting on Long-Pulse Operation of Fusion Devices, Vienna, Austria, October 2024
- Wilkie Choi, et al, "Simulation and experiment of EC steering of LH deposition on EAST", Invited talk at the 8th Asia-Pacific Conference on Plasma Physics, Malacca, Malaysia, Nov. 2024
- Wilkie Choi, et al, "Simulation and experiment of EC steering of LH deposition on EAST", Invited talk at the 66th Annual Meeting of the APS Division of Plasma Physics (2024). VI03.00001
- Shira Morosohk, J. Barr, M. Walker, N. Eidietis, A. Garofalo, S.H. Hahn, B. Xiao, Z. Luo, Q. Yuan, "Improvements to Shape Control Using Real-Time Optimization of Feedforward Coil

Current Trajectories", Poster Presentation at the 66th Annual Meeting of the APS Division of Plasma Physics (2024). PP12.00119

- Siye Ding, "Turbulence suppression in plasmas around the Greenwald density limit on EAST and DIII-D", Post-deadline Invited Talk at the 65th Annual Meeting of the APS Division of Plasma Physics (2023). NI02.00005
- S. Shi, et al, "Core heavy impurities control by ICRH on EAST", Oral Presentation at the US-EU Transport Task Force Workshop, Asheville, North Carolina, April 2024
- A.M. Garofalo, et al, "Progress in extending the DIII-D high-βP scenario to long pulse on EAST", Poster Presentation at the 65th Annual Meeting of the APS Division of Plasma Physics (2023). NP11.00083
- X. Gong, et al, "Overview of recent experimental results on EAST tokamak", Overview Oral at the 29th IAEA Fusion Energy Conference (FEC 2023), 16-21 October 2023, London, United Kingdom. IAEA-CN-316-2055
- M. Kotschenreuther, et al, "Novel methods to induce transport barriers and improve confinement", Poster at the 29th IAEA Fusion Energy Conference (FEC 2023), 16-21 October 2023, London, United Kingdom. IAEA-CN-316-2282
- Z. Wang, H. Wang, E. Schuster, Z. Luo, Y. Huang, Q. Yuan, B. Xiao, D. Humphreys, S.T. Paruchuri, "Implementation and Initial Testing of a Model Predictive Controller for Safety Factor Profile and Energy Regulation in the EAST Tokamak", poster presentation at 2023 American Control Conference (ACC), San Diego, CA, USA. May 31 - June 2, 2023
- Z. Wang, E. Schuster, X. Song, T. Rafiq, Y. Huang, Q. Yuan, Z. Luo, J. Barr, W. Choi, C. Holcomb, D. Humphreys, A. Hyatt, W. Wehner, "Model-based Feedback Control Design Towards Robust Realization and Sustainment of Advanced Scenarios in EAST", Poster Presentation at the 64th Annual Meeting of the APS Division of Plasma Physics (2022). CP11.00061
- A.M. Garofalo, et al, "High bP Research towards ITB Exploitation in a Fusion Reactor", Invited Plenary at the 18th International Workshop on H-mode Physics and Transport Barriers, Princeton University, September 2022
- C. Rea, J. Zhu, R. Granetz, K. Montes, R. Tinguely, R. Sweeney, N. Howard, P. Rodriguez-Fernandez, J. Barr, M. Boyer, K. Erickson, A. Maris, "Interpretable Machine Learning Accelerating Fusion Research", Tutorial Talk at the 64th Annual Meeting of the APS Division of Plasma Physics (2022). CT02.00001

3. MIT contribution (PI: P.T. Bonoli)

I. Introduction and Background

The principal goals of this project are to adapt high performance operating scenarios from DIII-D to the Experimental Advanced Superconducting Tokamak (EAST) in Hefei, China, develop the control physics understanding and solutions to enable this adaptation, and pioneer reactor-specific scenario and control solutions. Specific research objectives include the development of physics and control solutions necessary for demonstrating disruption-free long-pulse plasmas at high physics performance sustained simultaneously with the capability of handling the plasma exhaust and plasma-wall interactions using reactor-relevant materials surrounding the plasma. The Massachusetts Institute of Technology (MIT) contributes to these goals in the following task areas:

Task 1: Prediction and Demonstration of High Performance Steady-State Scenarios

This task focuses on developing the physics basis of fully non-inductive, high poloidal-beta (β_P) plasmas for application to steady-state high performance operating scenarios in ITER and Fusion Pilot Plants (FPPs). By optimizing at low plasma current and high plasma pressure, high-β_p operation reduces disruption risks and requirements on external current drive, while improving the energy confinement quality through Shafranov shift suppression of turbulence. In particular, this task aims to access on EAST the regime demonstrated on DIII-D [L. Wang et al, Nature Communications **12**, 1365 (2021)], which enables integration of high core performance with full detachment and small/no Edge Localized Modes (ELMs).

Task 2: Control for Disruption-free Scenario Realization and Robust Sustainment

This task focuses on the development and implementation of control algorithms and architectures required for the robust realization and sustainment of long-pulse advanced scenarios (see Task 1) while ensuring disruption-free operation. Reactor-grade challenges (superconducting coils, noisy/limited/non-magnetic diagnostics, divertor heat flux/temperature limits, etc.) arising in the control of both the magnetic configuration and the magnetic/kinetic state of the core plasma will be addressed by following a model-based approach.

II. Summary of Progress and Results

II.1. Task 1: Prediction and Demonstration of High Performance Steady-State Scenarios

Scope of Work: Our research efforts have focused on understanding and establishing lower hybrid current drive (LHCD) as a reliable RF actuator in developing high-performance, steady-state plasma scenarios on the EAST tokamak, which operates under a long-pulse, high-Z environment

that is scalable to reactor conditions. RF actuator optimization (particularly, reliable current profile control via off-axis LHCD at high-density) is crucial for accessing and sustaining advanced scenarios in RF-heated plasmas. An electron heating regime on EAST poses unique challenges in translating the high-β_p operation developed on DIII-D, which was developed with neutral beam power. Recent experiments and simulations on EAST provide pathways forward via plasma control and optimization, demonstrating a nearly doubling of T_i at a density approaching the Greenwald limit [Ding 2025]. RF actuators that can provide off-axis current drive are found to be crucial for reducing the magnetic shear at mid-radius for turbulence suppression. In the last three year project period, four major current drive research areas were investigated, including (1) modeling of velocity-space synergy effects for RF actuator optimization, (2) experimental quantification of lower hybrid power absorption in the H-mode plasmas, and (3) characterization of frequency-dependent parametric decay instabilities (PDIs) on EAST at a high density condition, including (4) an observation of intense PDIs in the "cold" branch of WEST L-mode plasmas, (5) an assessment of different fueling sources on LHCD efficiency, and (6) extension of non-inductive scenarios on EAST to higher magnetic field and plasma current. Our work contributes to the conceptual design of the LHCD system on the China Fusion Engineering Test Reactor (CFETR), which employs a PAM lower hybrid launcher concept with a source power of 20 MW at 4.6 GHz [Liu 2023].

II.1.1. RF Modeling of Synergy Interaction of Lower Hybrid Power with Electron Cyclotron Power

The availability of multiple RF actuators on EAST, as anticipated in a reactor, allows one to investigate the synergy effects in the RF current drive. Synergy current is the excess current that can arise from overlapping two wave-particle resonance regions in the velocity phase space. As available RF actuator powers are increasing with recent facility upgrades on EAST, it is of interest to quantify the synergy current fraction, which is often neglected in integrated modeling. Kinetic modeling analyses of the synergistic interaction between LHCD and electron cyclotron current drive (ECCD) have been conducted using the GENRAY/CQL3D ray-tracing/Fokker-Planck code package [Baek 2025]. This analysis incorporates the impact of collisional dissipation and fast-electron radial transport, which have been instrumental in reproducing the current profile in past EAST experiments. The effect of wave scattering by turbulence is examined phenomenologically by introducing an initial scattering angle due to interaction of the LH wave with the turbulence. The plasma discharge analyzed exhibits characteristics of the so-called "super I-mode" regime, i.e., formation of an internal temperature barrier in the core with a temperature pedestal at the edge [Song 2023]. Unlike a low-temperature, multi-pass damping regime, a high central temperature (Te0 ~6.5 keV) ensures spatial overlapping between LH and EC in the core region. The synergy current fraction is found to be 10-15% of the total current. Modeling also

predicts that the ECCD efficiency can be sustained at an off-axis location to a level comparable to on-axis ECCD when including the synergy current. Therefore, proper accounting for the phase space interaction will be essential for future scenario development, particularly for off-axis current drive in advanced scenarios. Modeling also suggests that the synergy effect could be utilized to improve the profile control capability of LHCD in a multi-pass damping regime. The research also provided input to the time-dependent TRANSP modeling of the LH-EC interaction by Dr. W. Choi at GA.

II.1.2. Quantification of Lower-Hybrid Power Absorption at a High Density

As plasma operation has been extended to high-density on EAST, a dedicated experiment to characterize lower hybrid power absorption was conducted at both frequencies (2.45 GHz and 4.6 GHz) in the high-density H-mode plasmas. The LHCD efficiency in the H-mode plasmas are generally found to be higher than in L-mode plasmas due to the higher temperature, and the efficiency up to 0.9×10^{19} A/W/m^2 with EC heating added at ~5.4×10^{19} m^{-3} (or the Greenwald fraction of ~0.75) [Li 2023]. The lower hybrid power absorption coefficient is evaluated using a break-in-slope analysis of the plasma kinetic and magnetic energies [Baek 2023]. The power absorption coefficient is found to be ~0.45 for 4.6 GHz at a high density (~4×10^{19} m^{-3}), which is higher than ~0.35 for 2.45 GHz. GENRAY/CQL3D modeling indicates that the observed level of power absorption can be accounted for by a combination of antenna spectrum, accessibility, and edge losses. While the antenna forward directivity is high at 75% for the 4.6 GHz passive-active multijunction (PAM) antenna, the effective power in the range of $1 < n_{\|} < 3$ is reduced to ~60%. Accessibility is found to be a dominant limiting factor over parasitic losses at 4.6 GHz for wave propagation and absorption in a high-density plasma. Antenna spectrum optimization may improve net power absorption. Indications of parasitic coupling, thought to originate from the damping of high-n// components in the spectrum, are observable. The LH power flow along the field line in the scrape-off layer plasma is observed with hot spots on the LH side limiter and on a distant limiter that is mapped to the LH antenna, emphasizing the importance of optimized power coupling in a reactor design.

II.1.3. Characterization of Lower Hybrid Parametric Decay Instabilities at Two Frequencies

EAST provides a unique environment where the frequency dependence of parametric decay instabilities (PDIs) can be investigated systematically with the LHCD systems at two frequencies (4.6 GHz and 2.45 GHz). Frequency spectral measurements show that the PDIs at 4.6 GHz are generally weak and are not expected to impact the current drive capability, unlike at 2.45 GHz. An RF magnetic probe array has been installed next to the 4.6 GHz LH side limiter to measure the variation in the wave parallel refractive index ($n_{//}$) [Yan 2023]. During a density ramp-up experiment, the dominant parallel refractive index ($n_{//}$) evaluated with the probe array increases

from the injected $n_{//} = 2.1$ to a higher value of $n_{//} = 3$, suggesting a possible upshift in wave $n_{//}$ by parasitic wave-edge interactions. A corresponding PDI onset of ion cyclotron quasi-modes is also observed, documenting the threshold density [Yan 2024]. The ion cyclotron sideband power remains low at ~40 dB below the pump power, and, therefore, it is not likely to play a critical role. At the same time, due to ion sound quasi-modes and/or wave scattering from turbulence, the degree of pump broadening also increases. The specific mechanism(s) responsible for this broadening cannot be definitively identified, but control of the edge/scrap-off layer density is emphasized. Meanwhile, the 2.45 GHz frequency spectrum indicates a high level of ion cyclotron PDIs, correlated with the anomalous loss of efficiency at high density. EAST plans to replace the 2.45 GHz system with a 4.6 GHz system [Gong 2024].

II.1.4. Observation of Lower Hybrid (LH) Parametric Decay Instabilities on WEST

A proof-of-principle spectral measurement of lower hybrid (LH) waves has been carried out during the C11 campaign on WEST using an RF Langmuir probe installed on the LH antenna. This is a part of the rescoping activities outlined in 2025 and has been coordinated with another RF research activity under the PSFC Cooperative Agreement (DE-SC0014264). The lower source frequency of 3.7 GHz on WEST, as compared to 4.6 GHz on EAST was expected to make it more susceptible to PDIs, but so far, the Tore Supra measurements indicate a weak level of PDIs at high density (50 dB below pump power). Interestingly, a unique phenomenon on WEST, is access to the "cold" branch induced by excess impurity tungsten radiation, resulting in a cold, dense plasma. In this unusually cold plasma, evidence of intense PDIs has been gathered. In a normal plasma (or "hot" branch with $T_{e0} \sim 2$ keV), only weak PDI sidebands are observed, consistent with the past Tore Supra report. However, with temperature collapse to below $T_{e0} \sim 1$ keV, sequential PDI transitions into ion cyclotron quasi-modes and non-resonant quasi-modes are observed. The spectrum is broad ($\Delta f \approx 300$ MHz), and dominated by harmonics of LH sidebands with a peak at the ~6th ion cyclotron harmonic. In some cases, the integrated sideband power can be comparable to the pump power. The current drive capability is expected to deteriorate significantly, and further RF modeling will be needed. The impurity boron dropper appears to help remain at the hot branch, and PDI signatures are absent. These observations will be reported at the upcoming APS-DPP Conference in Long Beach, CA (November 17-21, 2025).

II.1.5. Assessment of Fueling Source on LHCD Efficiency

A series of joint experiments were performed on EAST and Tore Supra/WEST to compare the impact of fueling location (HFS/LFS) and type [gas, pellets, supersonic molecular beam injection (SMBI)] on the efficiency of LHCD. The experiments on Tore Supra and WEST showed that fueling with pellets results in larger non-thermal electron populations at higher density (line averaged $n_e > 4\times10^{19}$ m^{-3}). Pellet fueling on Tore Supra/WEST is correlated with lower density

fluctuations in the edge plasma and lower neutral pressures in the vacuum chamber as compared with gas fueling at the same line averaged density. The results from EAST were less clear, with pellets not providing an obvious increase in fast electron bremsstrahlung. It should be noted that on EAST it was not possible to fuel only with pellets, but rather a mix of pellets and gas fueling was used in the experiment. With combined pellet/gas fueling, there was no measurable difference in torus neutral pressure as compared to gas only discharges. Although neither pellets nor SMBI were available on Alcator C-Mod, the results are consistent with published observations that the torus neutral pressure was more tightly correlated with LHCD efficiency as compared to line-averaged density [Wallace 2012].

II.1.6. Extension of Non-Inductive Scenarios to Higher Magnetic Field and Plasma Current

EAST has recently demonstrated a 1056-sec-long fully non-inductive discharge [Song 2023, Gong 2024], utilizing the 4.6 GHz system as a main current drive actuator (1.1 MW with additional EC of 0.55 MW), demonstrating the physics and engineering feasibility of the tokamak operation as a reactor. The plasma current was 300 kA and the line-averaged density was 1.8×10^{19} m^{-3}. Our experiments on EAST show that it is possible to sustain non-inductive discharges at higher magnetic field and plasma current than previously thought. The LH driven current was found to move farther off-axis by increasing from 2.5 T and 400 kA to 2.7 T and 450 kA. Experimental measurements show internal inductance (l_i) reducing from near 1 to about 0.8, indicating a significant broadening of the plasma current profile. Simultaneously, the loop voltage was sustained near zero despite an increase in line averaged n_e from 3 to 4×10^{19} m^{-3} indicating that the LHCD efficiency remains constant or even improves slightly. GENRAY/CQL3D analysis shows that the current profile peaks near r/a = 0.4 in the high field/high current discharge as compared to 0.2 in the reference scenario. This result suggests that it may be possible to sustain non-inductive discharges at higher field and current in a future FPP. A follow-up experimental proposal was submitted in 2024 to apply and assess the impact of applying early ECCD on the current profile broadening as a part of developing the high β_p scenario. This effort could be pursued in the future, if opportunities arise.

II.2. Task 2: Control for Disruption-Free Scenario Realization and Robust Sustainment

Scope of Work: Task 2 focuses on developing and implementing advanced control algorithms and system architectures to ensure the robust realization and sustainment of advanced, long-pulse plasma scenarios in fusion experiments. The objective is to maintain disruption-free operations despite the challenges posed by reactor-grade environments, including the use of superconducting coils, limited or noisy diagnostics, and strict divertor heat flux and temperature constraints. The task takes a model-based approach to controlling both the magnetic configuration and the magnetic

and kinetic state of the plasma core. The MIT team has focused on developing advanced modeling solutions on EAST, and on integrating efforts with both the local team as well as GA as part of development inside the Proximity Control architecture.

II.2.1. Advancements in Disruption Prediction Modeling

Building on previous efforts (2016-2021), the team continued to leverage EAST tokamak data to improve disruption prediction methodologies. A key outcome was the publication of an integrated deep learning (DL) model [Zhu 2022, Zhu 2023] that combines disruption prediction with the identification of multiple precursor events such as rotating and locked modes, H-to-L back transitions, and radiative collapses.

- The DL-based unstable event identifier, trained on 160 manually labeled DIII-D discharges, achieved an average 84% accuracy in identifying frequent unstable events.
- This model demonstrated the capacity to generalize to unseen discharges, effectively expanding the labeled dataset through automated annotation.
- Cross-machine prediction studies incorporating databases from Alcator C-Mod, DIII-D, and EAST showed improved predictive accuracy and longer lead times compared to baseline models.
- The model also exhibited strong qualitative performance in identifying events across different tokamaks, demonstrating promising cross-machine adaptability.

The MIT team has also contributed to the analysis of new EAST data, after the change to a full-metal-wall. Via transfer learning techniques [Guo 2023], the designed data-driven predictor (a multi-scale hybrid network) improves by ~17% reaching an AUC (Area Under the Curve) of 0.93.

II.2.2. Real-Time Disruption Prediction Implementation in EAST

The Disruption Prediction via Random Forest (DPRF) algorithm has been operational within the EAST Plasma Control System (PCS) starting 2020-2021, delivering real-time disruption forecasts within 150–250 microseconds [Rea-IAEA]. However, continued development and maintenance of DPRF slowed down during the 2023-2025 time frame, as travel to China and integration within the experimental team has become more complicated.

- DPRF integrates global plasma stability diagnostics (e.g., magnetic signals, HCN interferometer) with real-time equilibrium reconstruction parameters (e.g., internal inductance l_i, stored energy W_{mhd}, safety factor q_{95}, normalized beta β_N, and plasma elongation κ).
- The algorithm not only predicts imminent disruptions but also identifies the key drivers contributing to plasma instability, enhancing interpretability and control decision-making.

II.2.3. Corollary Research from Extended Team Members

- MIT graduate student Andrew Maris is conducting thesis research under the guidance of Dr. Cristina Rea, focusing on the prediction and avoidance of density limit disruptions. Early studies of the L-mode phenomenology used EAST data [Maris 2025]. However, due to lack of reliable diagnostics' coverage at the edge (0.85 < rho < 0.95), EAST data was removed from subsequent multi-machine study.
- In coordination with personnel funded under a different grant (DE-SC0024368), Matlab workflows instrumental to the development and assembly of "disruption_warning" databases were translated to python and absorbed in the DisruptionPy framework [https://zenodo.org/records/15359587, https://github.com/MIT-PSFC/disruption-py/].

II.2.4. Conclusion

Significant progress has been made in both the modeling and practical implementation of disruption prediction and avoidance strategies. The integration of advanced data-driven models and real-time control algorithms into experimental systems like EAST represents a critical step toward achieving disruption-free, reactor-relevant plasma operations. Future work was going to include updating the disruption warning databases with full-metal-wall experimental data to retrain the DPRF algorithm. Further efforts could have seen the final integration of DPRF with the Proximity Controller architecture in EAST PCS, alongside additional metrics for detecting the onset of $n=1$ tearing mode perturbations or the onset of the density limit pre-disruptive instabilities.

III. Publications

- [Baek 2025] S. G. Baek, M. H. Li, W. Choi, P. T. Bonoli, B. J. Ding, A. Garofalo, G. M. Wallace, M. Wang, H. Xu, Q Zang , and H. Zhao, "Modeling study of synergistic effects between lower hybrid and electron cyclotron current drive on EAST", Nuclear Fusion **65**, 056003. (2025)
- [Baek 2023] S. G. Baek, M. H. Li, P. T. Bonoli, B. J. Ding, G. M. Wallace, J. L. Chen, Y. M. Duan, X. Z. Gong, J. P. Qian, L. Wang, H. Yang, Q. Zang, J. Y. Zhang. and X. J. Zhang, "Experimental study of lower hybrid wave power absorption on EAST", AIP Conference Proceedings **2984**, 090004 (2023).
- [Ding 2025] S. Ding, A. M. Garofalo, H. Q. Wang, W. Choi, X. Z. Gong, J. P. Qian, J. Huang, D. Hatch, M. T. Kotschenreuther, S. Mahajan *et al*, "Turbulence suppression at extreme plasma densities on DIII-D and EAST", Physics of Plasmas. **32**, 052202 (2025).
- [Gong 2024] X. Gong, Y. Song, B. Wan, J. Li, W. Yuanxi, W. Xinchao, F. Liu, J. Chen, J. Hu, G. Xu *et al*, "Overview of recent experimental results on the EAST Tokamak", Nuclear Fusion **23**, 112013 (2024).

- [Guo 2023] B. H. Guo, D. L. Chen, C. Rea, M. Q. Wu, B. Shen, R. S. Granetz, Z. C. Zhang, Y. Huang, Y. M. Duan, and L. Zeng, "Disruption prediction on EAST with different wall conditions based on a multi-scale deep hybrid neural network", *Nuclear Fusion* **63** 09400 (2023).
- [Li 2022] M. H. Li, S. G. Baek, G. M. Wallace, B. J. Ding, C. B. Wu, G. H. Yan, P. T. Bonoli, M. Wang, L. Liu, L. M. Zhao *et al*, "Observation and analysis of lower-hybrid-current-drive density limit in EAST", Nuclear Fusion **62**, 126055 (2022).
- [Li 2023] M. H. Li, B. J. Ding, M. Wang, C. B. Wu, G. H. Yan, Z. G. Wu, S. Y. Lin, N. Yan, X. M. Zhai, J. L. Chen, X. J. Zhang, S. G. Baek, G. M. Wallace, P. T. Bonoli, J. P. Qian, J. Huang, and X. Z. Gong, "Lower hybrid current drive efficiency in H-mode plasmas on EAST tokamak," AIP Conference Proceedings **2984**, 090005 (2023).
- [Liu 2023] L Liu, Y. Yang, M. Li, L. Zhao, W. Ma, T. A. Zhou, C. Liu, M. Cheng, M. Wang, J. Shan, B. Ding *et al*, "Conceptual design of the LHCD system on CFETR", Fusion Engineering and Design **189**, 113444 (2023).
- [Maris 2025] A. D. Maris, C. Rea, A. Pau, W. Hu, B. Xiao, R. Granetz, E. Marmar, the EUROfusion Tokamak Exploitation Team,, the Alcator C-Mod Team, the ASDEX Upgrade Team, "Correlation of the L-mode density limit with edge collisionality", *Nuclear Fusion* **65** 016051 (2025).
- [Rea-IAEA] C. Rea, "Disruption Prevention via Interpretable Data-Driven Algorithms on DIII-D and EAST", 28th IAEA Fusion Energy Conference (FEC 2020). Virtual Event (May 10-15, 2021).
- [Song 2023] Y. Song, X. Zou, X. Gong, A. Becoulet, R. Buttery, P. Bonoli, T. Hoang, R. Maingi, J. Qian, X. Zhong *et al*, "Realization of thousand-second improved confinement plasma with Super I-mode in Tokamak EAST", Science Advances **9**, eabq5273 (2023).
- [Wallace 2012] G. M. Wallace, I. C. Faust, O. Meneghini *et al*, "Lower hybrid current drive at high density in the multi-pass regime", Physics of Plasmas **19**, 062505 (2012).
- [Yan 2024] G. H. Yan, B. J. Ding, C. B. Wu, M. H. Li, S. G. Baek, F. Napoli, T. T. Zhou, K. N. Geng, N. Yan, M. Wang, X. J. Zhang, H. D. Xu, J. H. Yang and W. Q. Ma, "Experimental investigation of PDI bifurcation of lower hybrid waves during electron density ramp-up in EAST", Nuclear Fusion **64**, 086018 (2024).
- [Yan 2023] G. H. Yan, B. J. Ding, M. H. Li, S. G. Baek, T. T. Zhou, C. B. Wu, J. H. Yang, N. Yan, M. Wang, X. J. Zhang, H. D. Xu, S. X. Wang, "Preliminary study of lower hybrid parametric decay instabilities under different heating schemes in EAST," AIP Conference Proceedings **2984**, 090006 (2023).

- [Zhu 2023] J. X. Zhu, C. Rea, R. S. Granetz, E. S. Marmar, R. Sweeney, K. Montes, and R. A. Tinguely. “Integrated deep learning framework for unstable event identification and disruption prediction of tokamak plasmas”, *Nuclear Fusion* **63**, 046009 (2023).
- [Zhu 2022] J. Zhu, “Data-driven predictive modeling of major disruptions and unstable event identification across multiple tokamaks” 6th Asia-Pacific Conference on Plasma Physics (October 9-14, 2022, Remote e-conference), Invited Talk MF1-114.

4. UCLA contribution (PI: D.L. Brower)

The primary UCLA goals for time period 2022-2025 were to:

1) Investigate Lower Hybrid Wave (LHW) deposition and current profile modification associated with LHCD using the POINT diagnostic system.
2) Measure magnetic fluctuations using POINT and directly determine the magnetic fluctuation-induced momentum flux, or dynamo effect, resulting from the correlated product of magnetic and pressure fluctuations.
3) Use POINT to directly determine the magnetic axis vertical position and integrate realtime output from this measurement into the EAST PCS for purposes of demonstrating non-inductive vertical position control under multiple magnetic divertor configurations.

I. LHW Current Deposition

In future fusion devices, lower-hybrid waves (LHWs) show great potential for plasma heating, current drive, and current profile modification. However, accurately determining the LHW deposition location through modeling alone remains challenging due to complex wave propagation within the plasma. To address this issue, a series of experiments were conducted on the Experimental Advanced Superconducting Tokamak (EAST) to investigate the effects of LHW on plasma current. Deposition location is directly determined from internal magnetic field measurements obtained using Faraday-effect polarimetry during the LHW modulation experiments. The "Amperian-loop" method provides a direct way to evaluate current deposition, and EFIT equilibrium constrained by polarimetry measurements can accurately evaluate current density profile changes induced by LHW injection. Good agreement was observed between simulation and measurement in identifying location and level of LHW current drive. Additionally, in experiments with plasma density ramp-up and LHW power step-up, the polarimetry system corroborated its capability to accurately determine current changes induced by LHWs. Results from these measurements are shown in Figure 15, where it is seen that the largest deposition is located approximately 30 cm above the plasma midplane, matching predictions from the GENRAY/CQL3D code.

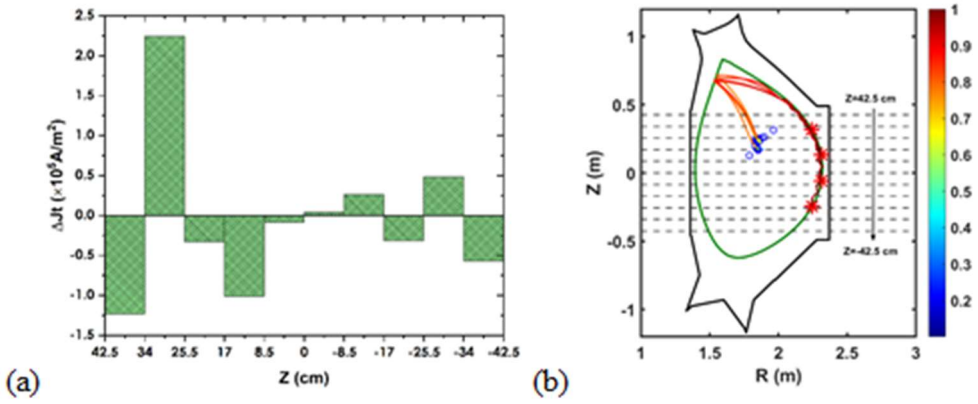

Fig. 15. (a) Relative change of toroidal current density between adjacent chords for plasmas with LHW-on and LHW-off) calculated by "Amperian-loop". (b) Maximum power deposition of LHW calculated by GENRAY/CQL3D code. The ray traces represent the propagation trajectories of the main absorption peaks from four antennas. The color scale represents the remaining power of the LHW, and the blue hollow circles indicate the primary deposition locations of the LHW, including both the main and secondary absorption peaks.

The POINT system is a Faraday-effect polarimeter-interferometer making measurements along 11 horizontal, vertically-displaced (8.5 cm) chords. Given the continuous change in the current distribution during LHW modulation, the moments just before the LHW input and the moments just after the final modulation pulse were selected for comparison to enhance clarity. Using these POINT data as an internal constraint in the EFIT code, q and current profiles can be calculated. Figure 16(a) and (b) show the line-integrated density and Faraday rotation angle profiles, respectively. Experimental data are represented by hollow symbols, while fitted data from the EFIT code are shown as solid symbols, indicating good agreement between the two. Figure 16(c) displays the q profile at 3 s and 5.3 s, with an enlarged view of the q range from 0 to 2 in the inner diagram. Sawtooth behaviour is consistently observed throughout the discharge, corresponding to q_0 values less than 1, as illustrated in Figure 16(c). The localization of sawtooth activity via SXR and ECE measurements enables the identification of the q=1 surface, providing results that align with those obtained from EFIT calculations. With LHW turned on, q_0 increases, and the core current decreases. The current increase due to LHW input predominantly occurs within region $0.3<\rho<0.5$, as depicted in Figure 16(d), which is consistent with the most pronounced current change position calculated by the "Amperian-loop" method. Deposition of LHW current is also calculated using GENRAY/CQL3D code for comparison. As shown in Figure 16(d), the calculated LHW current peaks at ρ about 0.35 which is consistent with measurement. The variation in toroidal current from EFIT does not precisely match the results calculated from the GENRAY/CQL3D code. This discrepancy may be attributed to the fast electron diffusion of LHW deposited current within the plasma and variations in the profiles of other current components.

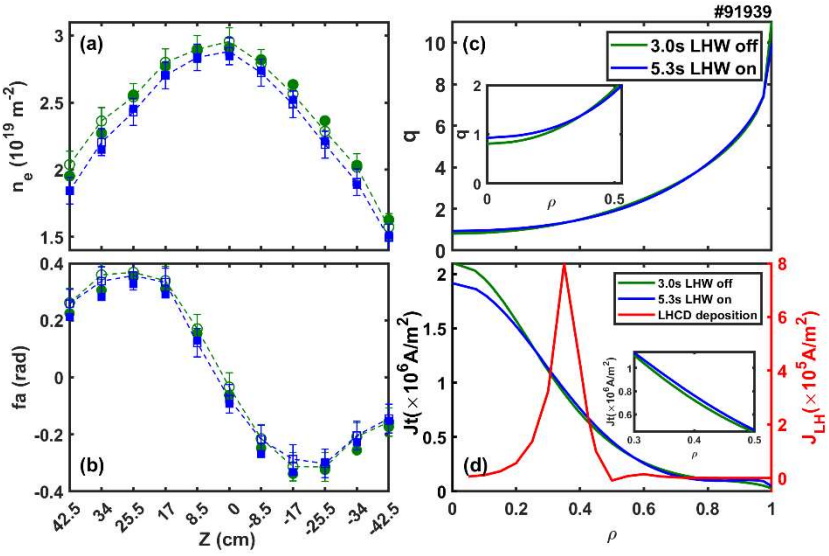

Fig. 16. (a) Line-integrated density and (b) Faraday rotation angle at 3.0 s (green) with LHW off and 5.3 s (blue) with LHW on. Hollow mark with dotted line is experimental data and solid mark is fitted data of EFIT code. (c) Safety factor q profiles and (d) current of these two moments calculated by the EFIT code by using POINT data as additional constraint. The red line is the calculated LHCD deposition by GENRAY/CQL3D code.

II. Magnetic Fluctuation Measurements

***Internal measurements of electromagnetic geodesic acoustic mode (GAM) in EAST plasmas*:** Electrostatic and electromagnetic features of geodesic acoustic mode (GAM) have been long observed by using multiple diagnostics such as reflectometry, Doppler backscattering system (DBS), external Mirnov coils. It is evident that $m = 1$ density fluctuations are indeed balanced by the compression of perpendicular flow fluctuations by combining up-down interferometer and DBS measurements on the midplane.

Multiple GAM fluctuating features have been measured during a long-pulse discharge in EAST simultaneously, including poloidal $E \times B$ flow $\tilde{v}_\perp$, density fluctuation $\tilde{n}_e$, internal magnetic fluctuations measured by Faraday-effect polarimeter for the first time, respectively. The ratio of $E \times B$ velocity fluctuation to the ion sound speed is $\tilde{v}_\perp/c_s \sim 0.01$. The GAM induced density fluctuations are proven to have a characteristic $m = 1$, with a maximum amplitude of approximately $\bar{\tilde{n}}_{e,GAM}/n_e \sim 0.29\%$. In addition, experiments have shown that the poloidal plasma flow compression is partially balanced by density fluctuations by combining up-down interferometer and DBS on midplane, which is the defining characteristic of GAM different from low frequency zonal flow.

Furthermore, internal magnetic fluctuations associated with GAM have been directly measured by laser-based Faraday-effect polarimetry for the first time. The experiment found that the magnetic fluctuation associated with GAM is surprisingly large, with a line-averaged

amplitude of $\frac{\tilde{\bar{B}}_{R,GAM}}{B_T} \sim 0.066\%$, the line-averaged magnetic fluctuations is significantly larger than 10^{-3} Gauss measured by edge coils. It is observed that internal magnetic fluctuations increase with β as expected from finite β . These observations offer a comprehensive understanding of the electrostatic and electromagnetic characteristics of GAMs (Geodesic Acoustic Modes). The presence of significant magnetic fluctuations may induce stochasticity in the field lines. Consequently, the propagation of sound waves along these stochastic field lines can mitigate flow damping, attributed to the short-circuit effect between adjacent flux surfaces[36]. Further experimental investigation is needed to elucidate the influence of magnetic fluctuations on plasma transport.

Fluctuation-Induced Dynamo Effect in a Magnetic Confinement Plasma: Electron temperature fluctuation-induced dynamo electric field has been measured in the core of high-temperature EAST tokamak plasmas by Faraday-effect polarimetry and electron cycle emission (ECE). It is found that a dynamo electric field primarily arises from the coherent interaction between radial magnetic field fluctuations and electron temperature fluctuations associated with the internal kink instability, acting to self-regulate the current profile to prevent sawtooth magnetic reconnection.

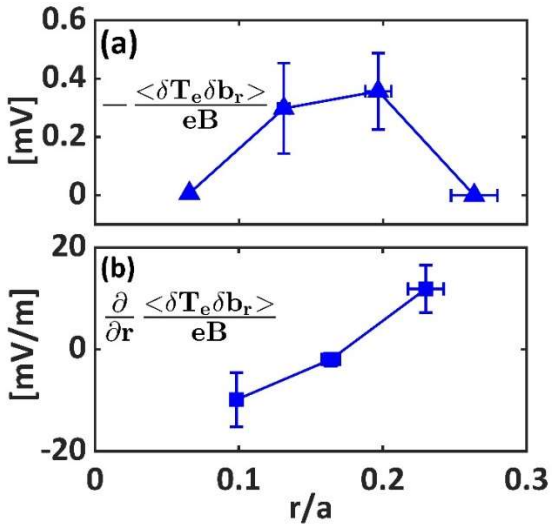

Fig. 17. Profiles of (a) mean correlated product $-\frac{<\delta T_e \delta b_r>}{eB}$*, and (b) temperature-fluctuation-driven diamagnetic dynamo* $\frac{\partial}{\partial r}\frac{\langle \delta T_e \delta b_r \rangle}{eB}$.

The experimentally measured fluctuation-induced dynamo profile is shown in Figure 17(b), determined by calculating the gradient of the electron momentum flux transport. The dynamo is -10mV/m inside the resonant surface and reverses sign when going across r_s, reaching a maximum of 12mV/m. The sign change arises from the fact that the correlated product, shown in

Figure 17(a), has a maximum near the resonant surface causing the gradient of the correlated product to change sign [Figure 17(a)]. The measured fluctuation-induced dynamo tends to reduce the total current inside resonant surface and acts to drive current outside. Hence, the fluctuation-induced dynamo electromotive force tends to transport current away from the plasma core towards the edge, similar to so called "flux pumping", thereby preventing current peaking near the magnetic axis. These results represent the first ever successful measurement of a fluctuation-induced flux, in this case the magnetic fluctuation-induced momentum flux, in the core of a high temperature tokamak plasma.

I. Non-Inductive Magnetic Axis Vertical Position Measurement and Control:

Vertical position stability plays a crucial role in maintaining safe and reliable plasma operation for long-pulse fusion devices. Vertical displacement events arising from the vertical displacement instability often lead to plasma disruption and can potentially cause damage to the device. Generally, the vertical position is measured using inductive magnetic coils installed inside the vacuum vessel, but integration drift effects are inherent for steady-state or long-pulse plasma operation. Developing a non-magnetic approach provides a fusion reactor relevant steady-state solution that avoids the negative impact of integration drift. On EAST, we compare the non-inductively determined vertical position made by line-integrated interferometer and polarimeter measurements to that employing inductive flux loop for a 1056 seconds H-mode discharge recently achieved on EAST (Experimental Advanced Superconducting Tokamak). Experimental results show that the non-inductive measurement is more robust than flux loops after 200 seconds if the integrator is not reset to suppress integrator drift.

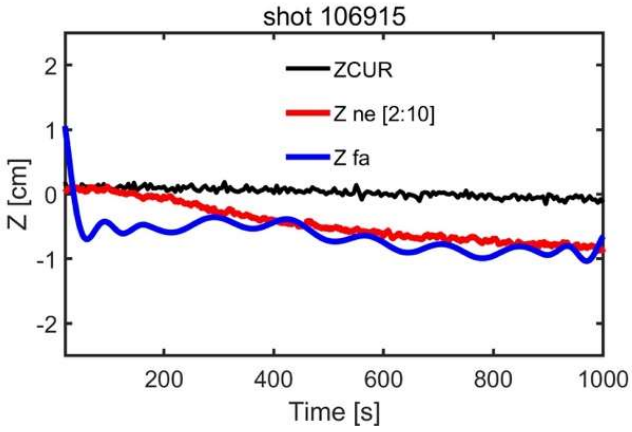

Fig. 18. Vertical position determined from magnetic flux loops (ZCUR-black line), and non-inductively measured from Faraday rotation (Z_fa-blue line) and plasma density centroid (Z_ne - red line) for 1000 second H-mode discharge on EAST.

The plasma vertical position can be determined from the magnetic axis position where the radial magnetic field is equal to zero. The horizontal POINT measurement chords are evenly

distributed across the poloidal cross section, consequently, POINT is able to determine the vertical position as the Faraday rotation angle should be zero when the probe beam propagates through the magnetic axis. The Faraday rotation angle equation can be expanded using Taylor equation for $Z/a \ll 1$.

$$\psi_F(Z) \approx \psi_F(Z_0) + (Z - Z_0)\frac{\partial}{\partial Z}\psi_F(Z) = 0 \quad (1)$$

Where the first order term is kept due to the proportionality of B_R to Z, Z_0 is the vacuum vessel midplane position which is typically defined as Z=0. Therefore, we have

$$Z_F = -\psi_F(0)/\psi_F(0)' \qquad (2)$$

$$\psi_F{}' \cong \Delta\psi_F/\Delta Z \qquad (3)$$

The equation above gives the center position of the innermost flux surface, Z_F, obtained directly from the line-integrated Faraday rotation measurement. The $\psi_F{}'$is calculated from the gradient $\Delta\psi_F/\Delta Z$ at $Z = 0$. The above relation can be evaluated for the 3 central POINT chords to give the vertical position, according to:

$$Z_F = 17 * \psi_F(0)/[\psi_F(-8.5cm) - \psi_F(8.5cm)] \quad (4)$$

The non-inductive vertical position measurement result using the POINT system is shown in Figure 18. The position determined from external magnetic probes combined with EFIT is indicated by the black line, the plasma density centroid uses signals for chords from Z=-34.0cm to Z=+34.0cm (9 chords) is shown with the red line and the vertical position from Faraday rotation is represented with the blue line. The non-inductive results from POINT measurements both show the plasma is moving down gradually during the course of the discharge. For the plasma density centroid, it is potentially influenced by SOL (Scrape Off Layer) area, however, the downward tendency is clear. The vertical position using Faraday rotation measurement indicates the plasma moves downward slowly, approximately 3mm, compared to the initial position measurement at the beginning of the discharge. This downward drift is not evident in the magnetic result, as it may potentially be impacted by the integration drifts, especially for long-pulse operation. One thing that should be pointed out is the inconsistency between Faraday rotation result and magnetic result at the beginning. This difference is mainly due to the impact of stray light error, which is a persistent system error in Faraday rotation angle measurement. This has been reported for polarimetry measurements in several devices like JET and RFX. Using an offline correction

method, the stray light error of Faraday rotation measurement on EAST can be reduced to approximately 0.5°. However, it still plays an important role in vertical position measurement with Faraday rotation signal. As shown in expression (5), we take the average Faraday rotation value at 100s for instance, the difference between calculation results of applying +0.5° and -0.5° is approximately 1.2 cm. This mainly contributes to the offset at the beginning of the discharge. In addition, a very low-frequency oscillation (~150 sec period) is also observed in Faraday measurement, which has been noted for the first time during long-pulse plasma operation. The source of this oscillation is unknown and more work will be performed to identify it during the next campaign. Combining these two errors together in Faraday rotation measurement, the vertical position measurement with Faraday rotation shows a difference with both the density and the magnetic results. But even with the impact from errors, the Faraday rotation result still indicates plasma slowly moves downward during the discharge.

Real-time vertical position control using non-inductive system was planned for an EAST experimental campaign but laser failure for POINT diagnostic prevented execution. Initial demonstration of non-inductive vertical position control was successfully made on the DIII-D tokamak by UCLA in January 2025.

III. Publications

- Y. Q. Chu, W. X. Ding, D. L. Brower, H. Lian, H. Q. Liu, Y. X. Jie, C. B. Wu, S. X. Wang, R. J. Zhu, Y. F. Jin, J. S. Geng, ***Investigation of LHW Current Deposition on EAST tokamak*, submitted to Nuclear Fusion; June, 2025.**
- W.Z. Mao, W.X. Ding, H.Q. Liu, A. Ti, D.L. Brower, H. Lian, Y.Q. Chu, L Zeng, H.L. Zhao, L. Zhang, J.P. Qian, Q. Zang, X.Z. Gong, L.Q. Hu, L.X.Xu, C. Zhou, T. Lan, A.D. Liu, J.L. Xie, G. Zhuang, Y.T. Song, B.N. Wan, J.G. Li and EAST team, *Fluctuation-Induced Dynamo Effect in a Magnetic Confinement Plasma*, Physical Review Research *5*, L022047 (2023).
- Y.H. Wang, W.X. Ding, C. Zhou, A.D. Liu, X. Feng, H. Lian, H.Q. Liu, Y.Q. Chu; D.L. Brower, W.Z. Mao, J.L. Xie, L.T. Gao, R.J. Zhu, X.M. Zhong, H.J. Ren, Z. Chen, W.X. Shi, S.F. Wang, *Internal measurements of electromagnetic geodesic acoustic mode (GAM) in EAST plasmas, Phys. Plasmas* 31, 092503(2024).
- H. Lian, H.Q. Liu, D.L. Brower, W.X. Ding, Y. Huang, S. X. Wang, W. M. Li, Y. Q. Chu, R. J. Zhu, and Y. X. Jie, *Non-Inductive Plasma Vertical Position Measurement for the 1056s Discharge on EAST*, Review of Scientific Instruments 93, 103511 (2022).

5. PPPL contribution (PI: Z. Sun)

I. Introduction

This report summarizes the research activities and key scientific findings accomplished by the PPPL collaboration under Task 3, "Power Handling and Core-Edge Integration," for the period of performance from 2022 to 2025. The primary objective of this task was to develop and integrate robust solutions for power exhaust, particle control, and edge stability in long-pulse, high-performance plasma scenarios on the EAST tokamak. The research successfully leveraged novel techniques, primarily impurity powder injection (Boron and Lithium), to address critical challenges for future fusion devices like ITER and Fusion Pilot Plants.

First, we developed and successfully implemented a novel dynamic wall conditioning technique combining feedforward and feedback control of lithium and Boron powder injection. This system provided unprecedented real-time control over fuel recycling and impurity influx, leading to the achievement of a record-breaking 1000-second H-mode discharge with remarkable stability. Second, our work established a clear synergistic benefit between impurity powder injection and RF heating, demonstrating that fresh Li and Boron (B) deposition can directly improve LHW core heating efficiency and increase plasma stored energy by up to 5-20%. Third, and most critically, we demonstrated two powerful pathways for integrated core-edge solutions. We developed a novel technique for on-demand ELM triggering using Li granules to actively expel core tungsten (W) impurities, reducing W-dominated radiation by up to 60% while simultaneously improving energy confinement by 30%. In a complementary approach, we achieved the first-ever demonstration of simultaneous ELM suppression and full divertor detachment using a synergistic combination of B powder and Neon (Ne) gas, providing a viable solution for managing both pedestal stability and divertor heat flux. Finally, we have advanced the fundamental physics understanding of these impurity-driven scenarios. Through systematic experiments reversing the toroidal magnetic field, we have unequivocally demonstrated the critical role of E×B drifts in determining divertor detachment asymmetry, plasma confinement, and the characteristics of the associated edge coherent modes. These complex experimental findings have been qualitatively validated by SOLPS-ITER and BOUT++ simulations, enhancing our predictive capability for next-step devices.

II. Project Activities, Findings, and Scientific Progress

II.1. Overview of Research Objectives and Approach

Our research, guided by the milestones in the Field Work Proposal (FWP-9982) and Task 3 of the grant narrative, aimed to address this challenge by developing and utilizing impurity powder/granule injection as an active, external actuator. The central hypothesis was that controlled

injection of low-Z materials (Li, B) could be used to either replace large ELMs with smaller, benign ones at high frequency or to modify the edge plasma conditions to access intrinsically ELM-stable regimes, all while contributing to power exhaust and real-time wall conditioning.

The research was structured to progressively:

1) Assess the plasma response to impurity powder injection, establishing it as a reliable tool for real-time wall conditioning and influencing ELM behavior.
2) Explore the underlying physics of ELM suppression and divertor radiation enhancement, focusing on the roles of turbulence and E×B drifts.
3) Optimize and integrate these techniques to sustain high-performance plasma operation with an attractive divertor, pedestal, and core solution.

To achieve these goals, we leveraged PPPL-developed hardware, including the Impurity Powder Dropper (IPD) and Impurity Granule Injector (IGI), on EAST.

II.2. Dynamic Wall Conditioning and Recycling Control for Record Long-Pulse Operation

Experiments successfully demonstrated that both Li and B powder injection can be used for active, real-time wall conditioning in long-pulse H-mode plasmas. The relationship between Li/B injection flowrate, D-alpha level, and wall retention is evaluated [Zuo, MRE 2023]. Experiments and SOLPS-ITER simulation indicate 60-90% B/Li deposits in the divertor region, depending on the plasma configuration. In the long-pulse time scale, the fuel recycling escalation and impurity buildup are characterized. We developed and implemented a novel feedforward-feedback integrated control system for the Li powder dropper [Wang, PST 2024]. This system utilizes a feedforward model based on pre-existing experimental data to establish a baseline injection rate, while a real-time feedback loop on the Li-II line emission signal—a reliable proxy for the Li flow rate—dynamically modulates the control voltage or D-alpha level to maintain stable wall conditions. This advanced control scheme allows the system to respond precisely to changing plasma conditions, ensuring a consistent and effective Li coating throughout the discharge. The achievement of a record 1000-second H-mode discharge unequivocally demonstrated the success of this technique [Sun, 8th ISLA, invited 2024], as shown in Figure 19.

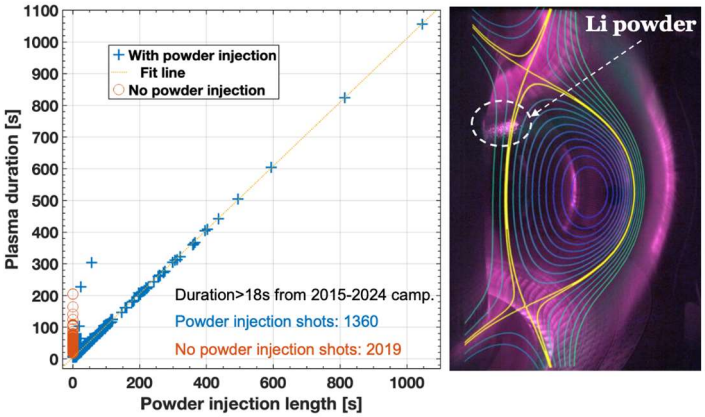

Fig. 19. Li powder injection applied to all long-pulse (>~220s) discharges in EAST, demonstrating that plasma duration is nearly equal to the injection time. This highlights the critical role of dynamic wall conditioning in extending H-mode operation to record lengths.

II.3. Synergistic Effects of Impurity Powder on RF Heating Efficiency

Experiments were conducted to assess how real-time wall conditioning impacts the efficiency of Lower Hybrid Wave (LHW) heating. The results showed a clear, positive synergy. In discharges with a passivated Li coating, the application of fresh Li deposition via powder injection led to a notable increase in the plasma stored energy by approximately 15%. This improvement was directly correlated with an increase in the core electron temperature, indicating more efficient power absorption from the LHW system. Subsequent injection of Boron powder into these discharges provided an additional ~5% increase in W_{MHD}. This finding is significant as it demonstrates that impurity powder injection can actively contribute to improved core plasma performance by creating more favorable conditions for RF power coupling and core heating.

II.4. Integrated Core-Edge Solutions: Simultaneous ELM Control, Divertor Detachment, and Tungsten Expulsion

The central goal of this research was to develop integrated solutions that simultaneously address the "core" problem of impurity accumulation and the "edge" problems of ELM-driven heat fluxes and divertor power handling. We successfully demonstrated two distinct but complementary pathways to achieve this integration. The first pathway focused on active impurity management by transforming ELMs from a problem into a solution. In otherwise ELM-absent EDA H-mode plasmas prone to severe W accumulation, we used the IPD to inject sub-millimeter Li granules into the upper X-point region. This technique achieved robust, on-demand ELM triggering with near 100% reliability. These externally-paced, small, and frequent ELMs proved remarkably effective at flushing tungsten from the plasma core [Sun, NF 2025]. We observed a reduction in W-dominated core radiation by up to 60%, which in turn allowed for a significant increase in energy confinement by up to 30%, as shown in Figure 20. This result establishes a novel control

method where small, benign ELMs can be triggered as needed to maintain core plasma purity without the damaging heat loads of large, spontaneous Type-I ELMs.

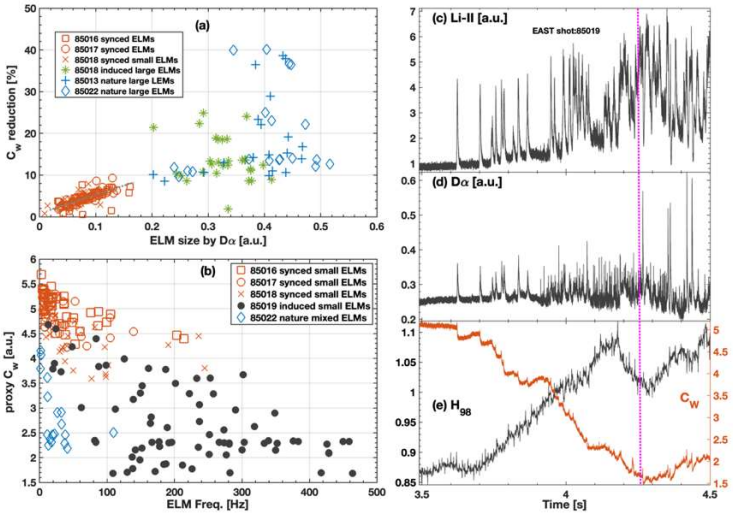

Fig. 20. Impact of ELM frequency and size on tungsten concentration and H98 factor. The data show that high-frequency, small ELMs triggered by Li granules (orange markers) achieve effective W control and high confinement, avoiding the large excursions of natural ELMs (blue/green markers).

The second pathway targeted a fully ELM-suppressed state compatible with divertor power exhaust. This was achieved through a synergistic combination of B powder injection and Ne gas seeding. While B powder alone effectively suppressed ELMs via the formation of an Edge Harmonic Mode (EHM), it only resulted in detachment of the inner divertor target with a favorable magnetic field direction. Conversely, Ne gas is an efficient radiator but can lead to core radiation issues and H-L back-transitions. By combining the two, we achieved a stable state with complete ELM suppression and significant detachment of both inner and outer divertor targets. The B powder stabilized the edge and conditioned the wall, allowing the plasma to tolerate the Ne radiation required for power exhaust without severe core contamination. This breakthrough, presented at [Sun, PSI, oral, 2024], demonstrates a viable integrated scenario for a reactor-relevant edge solution.

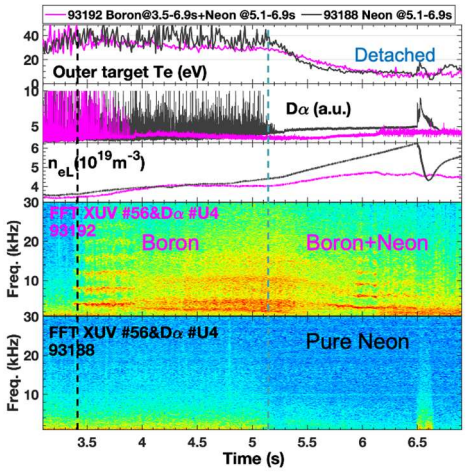

Fig. 21. Time evolution of key parameters for a discharge with combined B and Ne injection, compared with a pure neon injection at a lower rate. The data show energy detachment of the outer target (Te < 10 eV), suppression of ELMs, and the presence of an EHM, demonstrating a successfully integrated core-edge scenario.

II.5. Broadening the Small/No-ELM Operational Window and Advancing the Physics Understanding of Impurity-Driven Edge Scenarios

Our research successfully broadened the operational window for small or no-ELM regimes using B powder injection. We extended B-induced ELM suppression in Double-Null, Lower Single-Null plasmas and both magnetic field (Bt) directions. No edge harmonic mode is accompanied by ELM-suppressed LSN plasma with Boron injection from the top port. SOLPS-ITER simulation shows more Boron particles flow into the divertor for USN plasma compared to LSN plasma, as shown in Figure 22. ELM suppression in LSN plasma has a narrower range of the flow rate than the USN plasma.

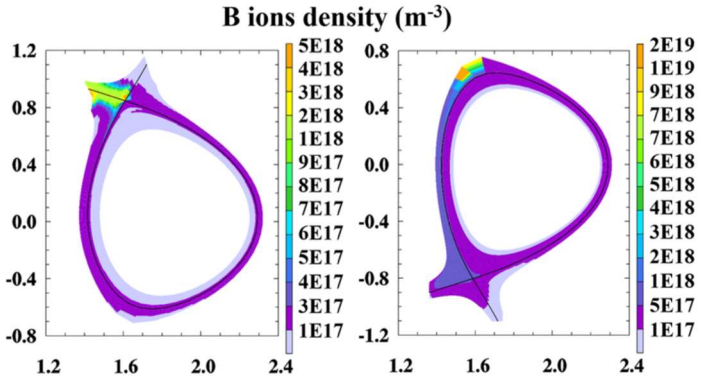

Fig. 22. Two-dimensional distribution of Boron ion density from SOLPS-ITER simulations for USN (left) and LSN (right) plasmas. The model shows a higher concentration of Boron in the divertor region for the USN case, consistent with experimental observations of divertor detachment asymmetries.

The B_T direction also fundamentally changed the outcome of B injection. With a favorable B_T (ion grad-B drift towards the X-point), we observed improved confinement, highly asymmetric

divertor detachment (inner target only), and a multi-harmonic EHM. With an unfavorable B_T, we observed slightly degraded confinement, more symmetric divertor detachment, and a different, single-frequency coherent mode. This clear dependence on B_T direction provides strong evidence for the critical role of E×B drifts in the SOL and PFR. These drifts act as a hidden actuator, asymmetrically transporting the injected boron and background plasma particles. This interpretation is strongly supported by qualitative agreement with SOLPS-ITER simulations, which reproduced the observed shift in detachment asymmetry by correctly modeling the drift flows [Peng, JoFE 2025].

Furthermore, our experimental results have been used to validate other critical simulation codes. The dynamics of ELM triggering by Li pellets were successfully modeled using the BOUT++ framework, showing good agreement with experimental observations of ELM evolution [Li, NF 2024&2025]. This close integration of experiment and validated simulation is crucial for building the predictive capability required to extrapolate these advanced scenarios to current devices and future fusion reactors.

III. Relevant Papers and Presentations

Papers:

- Z. Sun et al., Impact of toroidal field direction on integrated ELM-stable operation and divertor power exhaust via Boron powder injection in EAST, Nucl. Fusion, under review
- Z. Wang, Z. Sun et al., Fuel recycling and impurity characteristics under full metal wall and dynamic coated wall during long-pulse H-mode plasmas on EAST, Nuclear Fusion, under review
- Z. Sun et al., Active Impurity Control in ELM-absent H-mode Plasmas via On-Demand ELM Triggering with Lithium Granules Injection, 2025 Nucl. Fusion, accepted
- M. Li, Z. Sun et al., Simulation of Li-pellet triggered ELMs in EAST with an impurity model implemented under BOUT++ framework, 2025 Nucl. Fusion 65 026007
- W. Xu, Z. Wang, Z. Sun et al., Investigation of boron powder flow rates on real-time wall, Nuclear Materials and Energy 42 (2025) 101869
- L. Peng, Z. Sun et al., Role of E×B drift in divertor detachment control via boron powder injection on EAST, Journal of Fusion Energy, 2025, accepted
- Z. Wang, Z. Sun et al., Fuel recycling feedback control via real-time boron powder injection in EAST with full metal wall, Plasma Science and Technology, 2024, 125105
- L. Peng, Z. Sun et al., Comparative study of boron and neon injections on divertor heat fluxes using SOLPS-ITER simulations, Chinese Physics B 33 (11), 115201

- M. Li, T.Y. Xia, Z. Sun et al., Simulation of triggering and evolution of ELM by pellet injection in EAST under BOUT++ framework, 2024 Nucl. Fusion 64 086061
- J. Snipes, ... Z. Sun et al., Initial design concepts for solid boron injection in ITER, Nuclear Materials and Energy 41 (2024) 101809
- Z. Sun et al., Integration of ELM control with divertor detachment via Boron powder injection in EAST with tungsten wall, proceeding of IAEA-FEC 2023
- W. Xu, Z. Sun, et al., Active wall conditioning through boron powder injection compatible ELM control in EAST, Nuclear Materials and Energy (2023), 103159
- C. Liang, Z. Ma, Z. Sun, et al., Demonstration of object location, classification, and characterization by developed deep learning dust ablation trail analysis code package using plasma jets, Rev. Sci. Instrum. 94, 023506 (2023)
- G.Z. Zuo, Z. Wang, Z. Sun, et al., Deuterium recycling and wall retention characteristics during B powder injection in EAST, 2023 Materials Research Express 10 126402
- J.S. Hu, L. Li, G.Z. Zuo, Z. Sun, et al., A review of lithium application for the plasma-facing material in EAST Tokamak, Reviews of Modern Plasma Physics 7 (2023), 9

Presentations:

- Z. Sun et al., Simultaneous ELM Suppression and Divertor Detachment Combined Boron Powder and Ne Gas Injection In EAST, https://conferences.iaea.org/event/392/contributions/35950/, 30th IAEA Fusion Energy Conference (IAEA FEC 2025), October 13-18, 2025, Chengdu, China, Poster
- Z. Sun et al., Synergistic effect of Boron powder and Neon gas injection for power exhaust and ELM suppression in EAST with tungsten divertor, 26th International Conference on Plasma Surface Interaction in Controlled Fusion Device, 05.12-17, 2024, Marseille, France, Oral talk
- Z. Sun et al., The role of solid lithium injection in the achievement of record-duration high-performance plasmas in EAST, 8th International Symposium on Liquid Metals Applications for Fusion, 09. 8-12, 2024, Hefei, China, Invited talk
- Z. Sun et al., On-demand triggering of ELMs using impurity pellet injection into ELM-absent H-mode plasma on EAST, 19th International Workshop on H-mode Physics and Transport Barriers, September 24-27, 2024, Mito, Japan, Poster
- Z. Sun et al., Active Impurity Control in ELM-absent H-mode Plasmas via On-Demand ELM Triggering with Pellet Injection, 66th APS-DPP, October 7–11, 2024, Atlanta, Georgia, Poster
- Z. Sun et al., Integration of ELM control with divertor detachment via Boron powder injection in EAST with tungsten wall, 29th IAEA Fusion Energy Conference,16th-21st October 2023, London, UK, Poster

- Z. Sun et al., Effect of E×B on pedestal stability and divertor dissipation via Boron powder injection on EAST, 65th APS-DPP 10.30-11.3, 2023, Denver, CO, Poster
- Z. Sun et al., 'Improvement of plasma performance enabled by impurity powder injection in EAST', 23rd Workshop on Fine Particle Plasmas, remote, Dec. 17-18, 2022, Oral talk

6. LLNL contribution (PI: X.Q. Xu)

I. Introduction

Lawrence Livermore National Laboratory (LLNL) led Task 3, "Power Exhaust and Core-Edge Integration", of the GA-led EAST collaboration, focusing on the integration of power exhaust solutions with high-performance core scenarios for ITER and future fusion pilot plants (FPPs). LLNL's work combined advanced nonlinear BOUT++ simulations, UEDGE divertor modeling, turbulence theory, and machine-learning (ML) surrogate model development to address critical challenges in ELM control, SOL transport, and divertor detachment physics. The research was closely integrated with EAST long-pulse experiments and extended to cross-facility applications on DIII-D and ITPA joint experiments.

II. Technical Approach and Methodologies

LLNL employed an integrated approach, combining advanced fluid-based BOUT++ edge simulations, experimental validation using EAST discharges, and the development of ML-based surrogate models. Key methodological elements include:

- **BOUT++ edge and SOL turbulence simulations**:
  - Nonlinear six-field two-fluid simulations using BOUT++ to study edge stability, turbulence spreading, and ELM dynamics under EAST-relevant conditions.
  - Parametric scans over pedestal collisionality, density gradients, and electric field shear to probe ELM dynamics.
- **UEDGE detachment modeling**:
  - Large-scale parameter scans (>200,000 converged cases) spanning power input, impurity fraction, and diffusivity to classify detachment regimes.
  - Training of physics-informed neural networks on UEDGE datasets to enable near-real-time prediction of detachment behavior in EAST
- **Experiment–simulation integration**:
  - Cross-comparisons of simulation outputs with EAST pedestal, SOL, and divertor diagnostics; physics-based guidance for impurity seeding and small/grassy ELM regime access.

III. Scientific Contributions and Key Findings

III.1. Year 1 (FY23): Attached H-mode Plasmas and Surrogate Framework

- Characterized pedestal stability and transport in low collisionality, low gradient H-mode plasmas on EAST.
- Built initial surrogate model datasets from EAST-relevant UEDGE cases.

- Identified marginally unstable peeling modes as triggers for small ELMs, verified by BOUT++ simulations.

III.2. Year 2 (FY24): Detached Plasmas and Turbulence-Driven Broadening

- Demonstrated that fluctuation intensity flux (Γ_ε) correlates with SOL heat-flux width (λq) broadening in grassy/small ELM regimes.
- Conducted joint U.S.–China EAST impurity seeding experiments (Neon/Nitrogen, varied toroidal locations and injection rates) showing transitions from large to small/grassy ELMs, SOL broadening, and, with nitrogen, full divertor detachment.
- Applied EAST-derived turbulence metrics to DIII-D small ELM experiments and contributed to ITPA Pedestal and Edge Physics (PEP) activities.

III.3. Year 3 (FY25): Regime Control via Density Ratio and Zonal Flows

- Demonstrated that SOL width broadens in grassy and small ELM regimes due to outward turbulence entrainment.
- Confirmed that modifying pedestal Er profiles enables transitions from type-I ELMs to grassy regimes.
- Demonstrated, through BOUT++ simulations and experiments, that higher separatrix-to-pedestal density ratios on DIII-D suppress large ELMs by enabling continuous turbulence near the separatrix.
- Identified local ballooning mode dominance in high-SOL-density conditions on DIII-D, offering a predictive pathway to turbulence-saturated regimes.
- Identified fluctuation energy metrics as predictive tools for real-time control.
- Constructed a training dataset of over 200,000 UEDGE simulations for surrogate model development, with detailed evaluation presented in Section 4.
- Provided modeling guidance for ITPA PEP-DSOL-1 joint experiments, supporting ITER-relevant scenario optimization.

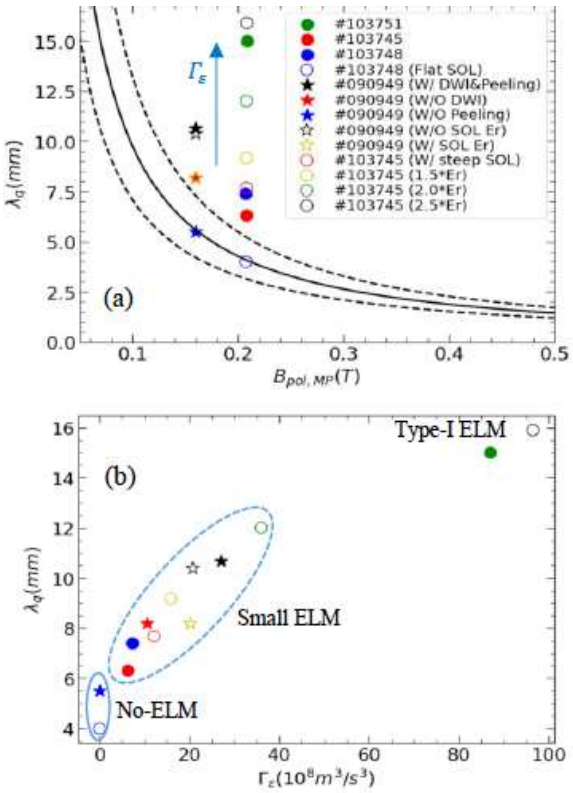

Fig. 23. Divertor heat flux width λq vs. (a) poloidal magnetic field at outer midplane βpol, MP and (b) fluctuation energy flux Γ_s for inter type-I ELMS (violet open circle and blue star), Type-I ELMs (Solid green and black open circle), and grassy ELMs (symbols within the dotted circle) from BOUT++ ELM simulations. Reproduced from Figure 3b in the work of Nami. Li et al, titled 'How fluctuation intensity flux drives SOL expansion', 2023 Nucl. Fusion 63 124005, with the permission of AIP Publishing.

These findings were further supported by BOUT++ simulations conducted for DIII-D, published in *Nuclear Fusion* (Li et al., 2025), and highlighted in DIII-D's Weekly Research Highlights (June 27, 2025). The study demonstrated that a higher separatrix-to-pedestal density ratio suppresses large ELMs by enabling continuous turbulence near the separatrix. Local ballooning modes dominate under high SOL density conditions, offering pathways to small ELM or turbulence-saturated regimes. These insights contribute directly to ITER-relevant control strategies for ELM mitigation and edge turbulence regulation.

As part of this effort, LLNL strategically redirected a portion of EAST-focused modeling to support small ELM physics on DIII-D. This included providing simulation guidance to Dr. Brian Victor's experiments on *Experimental Advances in QCE-like Small ELM Regimes*. The work led to one peer-reviewed publication (Nami Li *et al.*, *Nucl. Fusion* **65**, 076023 (2025)), two invited APS-DPP 2025 talks by (Brain Victor and Nami Li), and two oral presentations at IAEA FEC 2025 (by Nami Li and Filippo Scotti). This cross-facility synergy highlights the broader scientific impact of EAST-derived innovation on U.S. tokamak platforms.

IV. Simulations, Experiments, and Diagnostics

Simulations (see Figures 23 and 24) demonstrated SOL heat flux width (λ_q) dependence on poloidal magnetic field and Γ_ε. EAST data compared with BOUT++ predictions confirmed trends in fluctuation-induced SOL broadening. Diagnostics linked Er shear, turbulence modes, and zonal flows to ELM dynamics.

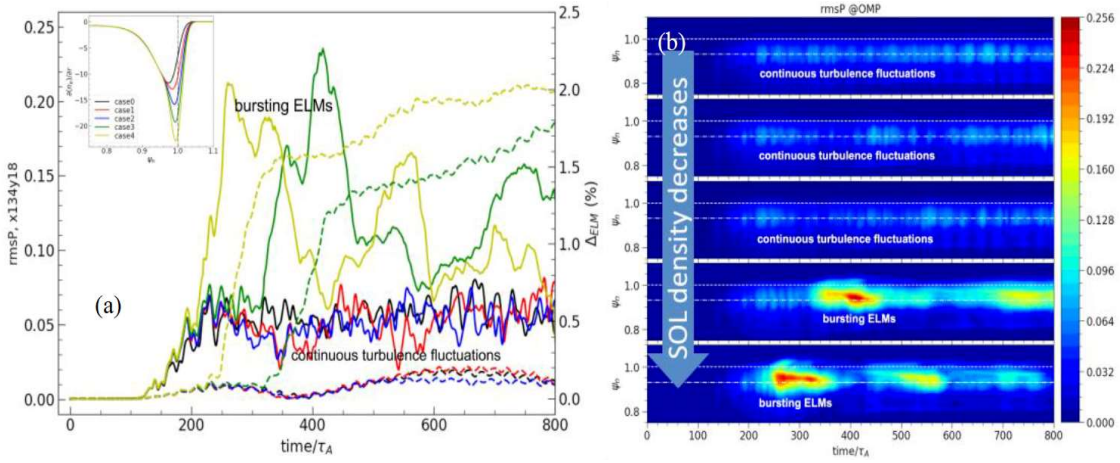

Fig. 24.(a) Time evolution of the RMS value of pressure fluctuations at OMP and peak pressure gradient location (solid curves), along with ELM sized (dashed curves) for SOL density scan. The corresponding density gradient for the scan is shown in the inset plot. (b) 2D spatial-temporal evolution of RMS value of pressure fluctuations at OMP.

In FY24, LLNL led a U.S.–China joint experiment on EAST (conducted May 31 and June 5, 2024) to investigate impurity seeding effects on ELM mitigation, SOL broadening, and divertor detachment. Building upon BOUT++ and UEDGE predictions of turbulence-driven fluctuation

entrainment and enhanced transport, the experiment varied Neon and Nitrogen seeding at different toroidal locations and injection rates. Key findings included a successful transition from large to small ELMs, significant SOL broadening, and, in the case of nitrogen, reaching plasma detachment. These results support the viability of impurity-seeded small/grassy ELM regimes for next-generation long-pulse tokamak operation. The findings were presented at the 2025 ITPA Pedestal and Edge Physics (PEP) meeting and are currently under further analysis and simulation validation by our EAST collaborators. This work exemplifies the integrated modeling and experiment approach central to the EAST collaboration and supports design optimization for devices such as ITER and CFETR.

IV.1. UEDGE Simulation Campaign and Neural Network Surrogate Development

As part of LLNL's contribution to EAST modeling, a large-scale parameter scan was performed using the UEDGE code to explore density detachment behavior. These simulations covered a wide range of parameter traversals (e.g., power input, impurity fraction, diffusivity). A total of over **400,000 usable 2D UEDGE solutions** were generated, with a convergence rate of over 70%. These scans informed classification of detachment regimes (attached, rollover, detached) and provided physically diverse training data for machine learning models. Development and refinement of ML-based surrogate models for EAST divertor scenarios are ongoing, led by EAST collaborators, with a focus on enhancing fidelity and physics consistency.

These efforts underscore LLNL's leadership in high-throughput simulation, ML surrogate modeling, and EAST-relevant detachment physics—supporting long-pulse scenario design and real-time control development.

V. Publications and Scientific Output

- 14 peer-reviewed papers.
- 10+ invited talks, including PSI-26 (2024), AAPPS-DPP (2023), APS-DPP (2022, 2024), Sherwood Theory conference (2023) and TTF workshops (2023, 2024, 2025).
- *Latest upcoming Invited and Oral Presentations as leading speaker and leading co-authors*
  - Nami Li: Invited Talk, APS-DPP 2025 — "Controlling ELM Dynamics: From Bursting Instabilities to Continuous Turbulence"
  - Nami Li: Oral Presentation, IAEA FEC 2025 — Chengdu, China
  - Brian Victor: Invited Talk, APS-DPP 2025 — "Experimental Advances in QCE-like Small ELM Regimes"
  - Filippo Scotti: Oral Talk, IAEA FEC 2025 — "Core-Edge Integration for Negative Triangularity Scenarios"

This work has culminated in multiple high-impact publications, including two recent *Nuclear Fusion* papers analyzing DIII-D and EAST pedestal turbulence and SOL transport [Li et al., NF 65 (2025) 076023; Zhang et al., NF 65 (2025) 056019]. In recognition of the scientific excellence emerging from this project, Dr. Nami Li received the 2024 LLNL Director's Excellence in Publication Award for her lead-author paper, *"How fluctuation intensity flux drives SOL expansion"* (*Nucl. Fusion* 63, 124005, 2023). The award honors her groundbreaking contribution to advancing the understanding of turbulence-driven scrape-off layer (SOL) broadening—an insight critical for controlling edge transport in future fusion reactors. Conducted as part of the EAST collaboration and developed in partnership with the BOUT++ and ABOUND SciDAC teams, this work exemplifies LLNL's leadership in boundary plasma physics and highlights the impact of U.S.–China collaboration on long-pulse scenario development.

In addition, LLNL's findings on grassy ELM regimes and turbulence spreading contributed to two major ITPA-led community reviews: the Edge and Pedestal Physics chapter [Fenstermacher et al., *Nucl. Fusion* 65 (2025) 053001] and the Scrape-Off Layer and Divertor Physics chapter [Krieger et al., *Nucl. Fusion* 65 (2025) 043001], where BOUT++ simulations of turbulence-driven broadening of the divertor heat flux width were prominently featured (see Figure 24). These contributions underscore LLNL's central role in shaping ITER-relevant understanding of SOL transport and ELM control.

VI. Broader Impacts and Future Directions

LLNL's integrated modeling and experiment strategy delivered:

- **Predictive metrics** ($\Gamma\varepsilon$) for turbulence-driven SOL broadening, representing a shift from classical scaling laws toward turbulence-based transport models.
- **Large-scale dataset** (>200,000 UEDGE cases) for training high-throughput, physics-informed surrogate models, enabling real-time detachment prediction and control.
- **Validated impurity-seeding approaches** for sustaining grassy/small ELM regimes with full detachment in long-pulse operation.
- **Cross-facility application** of EAST innovations to DIII-D experiments and ITER-relevant scenario planning via ITPA community reviews.

These advances position LLNL as a leader in uniting advanced boundary plasma physics with operational control strategies for next-generation fusion devices. Looking ahead, the integrated framework—spanning BOUT++, UEDGE, ML surrogates, and experimental validation—offers a scalable toolchain for optimizing edge–SOL–divertor physics in ITER-class devices. The surrogate models and predictive metrics will be applied to closed-loop detachment control, while

ongoing collaborations—from EAST to KSTAR and DIII-D —will continue driving progress in long-pulse operational strategies for future reactors.

VII. Publications and Talks (FY23–FY25)

- Li, Nami; Xu, Xueqiao; Victor, Brian; Li, Zeyu; Wang, H, Exploring the Transition from continuous turbulence fluctuations to bursting ELMs in High SOL Density Regimes, Nucl. Fusion 65 (2025) 076023.
- *T. Zhang, F.F. Long, G.S. Li, X.Q. Xu, J.B. Liu, K.N. Geng, Y.F. Wang,B. Zhang, K.X. Ye, Z.Q. Zhou, F.B. Zhong, F. Wen, N. Yan, X. Gao, and the EAST team, Observation of pedestal mode spreading into SOL and broadening of divertor particle flux width on EAST tokamak, Nucl. Fusion 65 (2025) 056019.*
- X.Q. Xu, N.M. Li, M.L. Zhao, P. H. Diamond, X. Liu, G. S. Xu, B. Zhu, T. D. Rognlien, ”Fluctuation Entrainment and SOL Width Broadening in Small/Grassy Regime”, Nuclear Materials and Energy 101866 (2025).
- X. Lin; Q. Q. Yang; G. S. Xu; G. Z. Jia; C. Zhang; Y. F. Wang; N. M. Li; N. Yan; R. Chen; X. Q. Xu; H. Y. Guo; L. Wang; S. C. Liu; Q. Zang; T. Zhang ; F. B. Zhong; Y. F. Jin; Edge-localized mode mitigation enabled by active control of pedestal density gradient with new EAST tokamak divertor; Phys. Plasmas 32, 012503 (2025).
- Nami Li, X.Q. Xu, B.S. Victor, Z.Y. Li and H.Q. Wang, Transition from Continuous Turbulence Fluctuations to Bursting ELMs in High SOL Density Regimes. The 30th IAEA Fusion Energy Conference (FEC2025).
- Fenstermacher, Max; Snyder, Philip; Osborne, Thomas; Saarelma, Samuli; Maingi, R; Dunne, Mike; Wolfrum, Elisabeth; Frassinetti, Lorenzo; Hughes, Jerry; Huijsmans, Guido; Park, Gunyoung; Sheikh, Umar; Urano, Hajime; Zhang, Tao; Laggner, Florian; Kirk, Andrew; Labit, Benoit; Paz-Soldan, Carlos; Futatani, Shimpei; de la Luna, Elena; Viezzer, Eleonora; Gil, Luís; King, Jacob; Liu, Zixi; Xu, Xueqiao; Diallo, Ahmed; Groebner, Richard; Cathey, Andres; Hoelzl, Matthias; Suttrop, Wolfgang; Vanovac, Branka; Becoulet, Marina; Liu, Yueqiang; Baylor, Larry; Lang, Peter; Lunsford, Robert; Wilcox, Robert; Wingen, Andreas; Kim, Sunhee; Burrell, Keith; Chen, Xi; Nelson, Andrew; Happel, Tim; Progress in Pedestal and Edge Physics, Chapter 3 of the Special Issue: On the Path to Tokamak Burning Plasma Operation", Nucl. Fusion 65 (2025) 053001.
- D. R. Zhang, R. Ding, H. Si, Y. P. Chen, X. Q. Xu, T. Y. Xia; Turbulence simulations with BOUT++ by using SOLPS grids for SOLPS/BOUT++ coupling, Contrib. Plasma Phys. 2024; 64:e202300152.
- N. Li, X.Q. Xu, P.H. Diamond, Y.F. Wang, X. Lin, N. Yan, and G.S. Xu, , Journal of Plasma Physics 90, 905900117 (2024)

- N. M. Li, X. Q. Xu, P. H. Diamond, T. Zhang, X. Liu, Y.F. Wang, N. Yan and G. S. Xu, "How fluctuation intensity flux drives SOL expansion", Nucl. Fusion 63 (2023) 124005
- X.X. He, X.Q. Xu, Z.Y. Li, B. Zhu, and Y. Liu, , Nucl. Fusion 62, 056003 (2022). .
- X.Q. Xu, , Science China Physics, Mechanics & Astronomy 65, 235231 (2022),
- W. Lin, X. Wang, X. Xu, D. Kong, Y. Wang, J. Chen, Z. Wang, and C. Xiao, , Plasma Sci. Technol. 24, 055103 (2022).
- Nami. Li , X.Q. Xu, Y.F. Wang, N. Yan, J.Y. Zhang, J.P.Qian, J.Z. Sun and D.Z. Wang, , Nucl. Fusion 62, 096030 (2022).
- Nami Li, X.Q. Xu, Y.F. Wang, X. Lin, N. Yan, and G.S. Xu, , Phys. Plasmas 29, 122302 (2022).

VIII. Plenary/Invited Talks (FY23–FY25)

- X.Q.Xu, Jianyi LI, Nami Li, "Impact of High-Z Impurities on Turbulence and ELM Stability: Insights from Advanced Two-Fluid and GLF Models", 2025 US Transport Task Force Workshop (TTF), Seattle, Washington, on April 22-25, 2025.
- Nami Li, "BOUT++ simulations of small ELM dynamics, including zonal flows and fields", "Turbulence Entrainment in negative triangularity configuration & ELMs", ABOUND SciDAC Team Meeting & BOUT++ Workshop, August 5-9, 2024, Livermore, CA, USA
- Xueqiao Xu, BOUT++ Physics Development, 2024 ABOUND SciDAC Team Meeting & BOUT++ Workshop, Livermore California, USA
- X.Q.Xu, Nami Li, M. L. Zhao, et al., "Fluctuation Entrainment in Tokamak Scrape-Off Layers: Implications for SOL Width and Detachment", The 26th International Conference on Plasma Surface Interaction in Controlled Fusion Devices (PSI-26) May 12-17th, 2024, Marseille, France
- X.Q.Xu, Nami Li, "Fluctuation Entraining, SOL Width Broadening and Divertor Plasma Detachment in Small/Grassy Regime", 2024 US Transport Task Force Workshop (TTF), Asheville, North Carolina, USA, April 9-12, 2024,
- Nami Li, "BOUT++ Simulations on Turbulence Spreading in Small ELM Regimes for Divertor Heat Load Control", 2023 Sherwood Fusion Theory Conference, Knoxville, Tennessee, USA May 8-10,2023,
- Nami Li, "Small ELM dynamics and its impact on the SOL width scaling", BOUT++ 2023 workshop, Livermore, CA, USA, January 9-11, 2023
- Nami Li, "Width Expansion driven by Fluctuation Energy Intensity Flux", AAPPS-DPP 2023 Annual Conference, Nagoya, Japan, November 13-17, 2023
- Nami Li, "On the dual merits of small ELMs", 2023 US Transport Task Force Workshop (TTF), Madison, Wisconsin, USA, May 2-5, 2023,

- Nami Li, X.Q. Xu P. H. Diamond, Y.F. Wang, X. Lin, N. Yan and G.S. Xu, “Small ELM dynamics and its impact on SOL width broadening”, 64th Annual Meeting of the APS Division of Plasma Physics, October 17-21, 2022, Spokane, WA USA.


GENERAL ATOMICS